

Role of Arc Processes in the Formation of Continental Crust

Oliver Jagoutz¹ and Peter B. Kelemen²

¹Department of Earth, Atmospheric and Planetary Sciences, Massachusetts Institute of Technology, Cambridge, Massachusetts 02139; email: jagoutz@mit.edu

²Department of Earth and Environmental Sciences, Lamont-Doherty Earth Observatory, Columbia University, Palisades, New York 10964; email: peterk@ldeo.columbia.edu

Annu. Rev. Earth Planet. Sci. 2015. 43:363–404

First published online as a Review in Advance on March 23, 2015

The *Annual Review of Earth and Planetary Sciences* is online at earth.annualreviews.org

This article's doi:
10.1146/annurev-earth-040809-152345

Copyright © 2015 by Annual Reviews.
All rights reserved

Keywords

continental crust, oceanic arc, subduction zone, magmatism, delamination, relamination

Abstract

We review data and recent research on arc composition, focusing on the relatively complete arc crustal sections in the Jurassic Talkeetna arc (south central Alaska) and the Cretaceous Kohistan arc (northwest Pakistan), together with seismic data on the lower crust and uppermost mantle. Whereas primitive arc lavas are dominantly basaltic, the Kohistan crust is clearly andesitic and the Talkeetna crust could be andesitic. The andesitic compositions of the two arc sections are within the range of estimates for the major element composition of continental crust. Calculated seismic sections for Kohistan and Talkeetna provide a close match for the thicker parts of the active Izu arc, suggesting that it, too, could have an andesitic bulk composition. Because andesitic crust is buoyant with respect to the underlying mantle, much of this material represents a net addition to continental crust. Production of bulk crust from a parental melt in equilibrium with mantle olivine or pyroxene requires processing of igneous crust, probably via density instabilities. Delamination of dense cumulates from the base of arc crust, foundering into less dense, underlying mantle peridotite, is likely, as supported by geochemical evidence from Talkeetna and Kohistan. Relamination of buoyant, subducting material—during sediment subduction, subduction erosion, arc-arc collision, and continental collision—is also likely.

1. ROLE OF ARC CRUST IN CONTINENTAL GENESIS AND EVOLUTION

Earth is unique among all rocky planets in that it has developed a clear bimodality in the characteristics of its outmost solid layer, the crust. Earth's solid surface is characterized by the low-lying oceanic crust (on average 3.7 km below sea level) and the highstanding continental crust (on average 0.8 km above sea level) (Eakins & Sharman 2012). Besides this obvious topographic expression, oceanic crust and continental crust differ systematically in multiple aspects. Oceanic crust is generally less than 8 km thick and younger than ~ 200 Ma, as older oceanic crust gets recycled back into the upper mantle along subduction zones. In contrast, continental crust is ~ 40 km thick and has a diverse age structure, with rocks older than 4 Ga preserved locally. The pronounced difference in topographic expression and preservation potential reflects a difference in composition: Whereas oceanic crust is basaltic ($\sim 50\%$ SiO_2), bulk continental crust is andesitic ($\sim 60\%$ SiO_2). Geochemical data, and the present-day composition of lavas in different tectonic settings, indicate that continental crust formed in subduction-related volcanic arcs, or via a geochemical process very similar to the arc magmatic process today (**Figure 1**).

Accordingly, a well-known continental crust paradox has long been articulated as follows: (a) Geochemical similarity and uniformitarian plate-tectonic interpretations indicate that continental crust is mainly formed via arc magmatism (**Figure 1**). (b) The net flux from the mantle into arc crust has the composition of a primitive basalt, with $<52\%$ SiO_2 and Mg\# [molar $\text{Mg}/(\text{Mg} + \text{Fe})$] >0.65 . (c) Continental crust is andesitic to dacitic, with $56\text{--}66\%$ SiO_2 , Mg\# $0.43\text{--}0.55$, and other compositional features characteristic of intermediate composition, calc-alkaline magmas. Accordingly, either the net flux from the mantle in subduction zones is more evolved than basaltic and/or additional mechanisms are important to transform the basaltic mantle-derived melts into andesitic continental crust.

The aims of this article are (a) to review data and ideas concerning the bulk composition of volcanic and plutonic arc crust and (b) to discuss proposed mechanisms that could help solve the

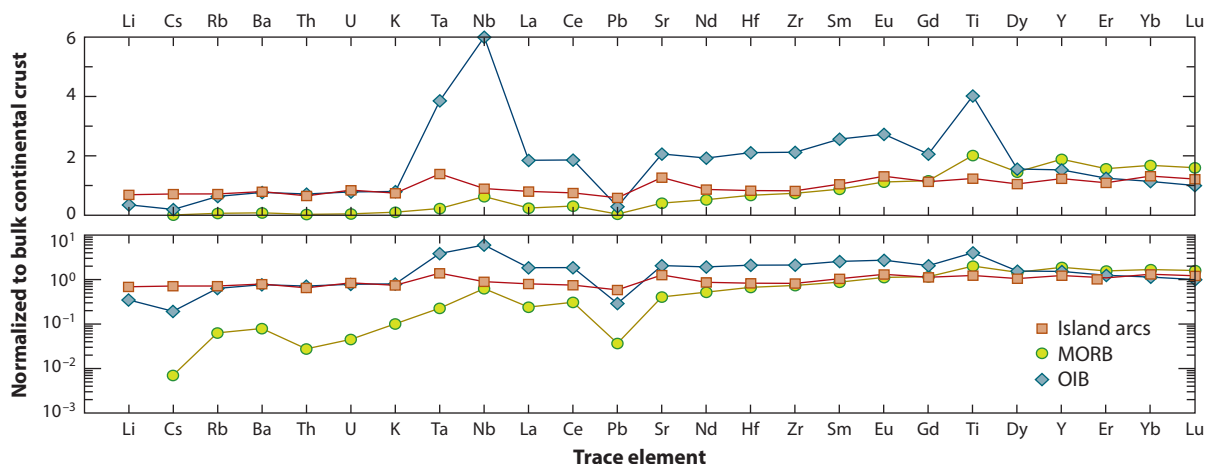


Figure 1

Extended trace element diagram normalized to bulk continental crust composition (Rudnick & Gao 2004, 2014), showing the average trace element systematics of volcanic rocks from oceanic ridges [mid-ocean ridge basalts (MORB); PetDB (<http://www.earthchem.org/petdb>), accessed 2005], ocean island basalts (OIB; McDonough & Sun 1995), and island arcs [B. Gunn's compilation (<http://www.geokem.com>)]. The trace element systematics of bulk continental crust are essentially identical to those of arc volcanics, strongly suggesting that continental crust is formed in subduction zones.

continental crust paradox. Our review is guided by the hypothesis that arc processes are central to the creation and evolution of continental crust. Recent work has strengthened this hypothesis, which suggests that other proposed processes play a comparatively minor role.

We focus on new data on plutonic rocks in intraoceanic arc crustal sections. Arc plutonic rocks are mainly exposed in accreted arc terranes that have undergone uplift and erosion, exposing middle and lower crustal intrusive rocks from beneath their volcanic and volcanoclastic carapace. In particular, the Cretaceous to Eocene Kohistan arc section in northwest Pakistan and the Jurassic Talkeetna arc section in south central Alaska contain plutonic rocks from a wide spectrum of crustal depths extending down to the seismic Moho and the petrologic crust-mantle transition zone. Less complete sections, mainly composed of mid-crustal, felsic plutonic rocks, extend east from Kohistan into the Ladakh batholith and west from Talkeetna into the Alaska Peninsula batholith. There are few plutonic rocks exposed in most active oceanic arcs. Although xenoliths and seismic data reveal their presence at depth, they are covered with a carapace of volcanic and volcanoclastic debris. An important exception is the Aleutian arc, where abundant intermediate to felsic plutonic rocks are exposed.

Our review is largely focused on quantitative geochemical and seismic data, informed by petrologic estimates of mineral equilibration pressures and temperatures. The recent reviews of the geology of arc crust by DeBari & Greene (2011) and Burg (2011), which contain much more information on mineralogy, rock textures, and intracrustal differentiation processes, provide wonderful complements to our approach.

2. TWO “COMPLETE” ARC CRUSTAL SECTIONS

2.1. Talkeetna Arc Crustal Section, South Central Alaska

Here we briefly review the lithological composition of the Talkeetna arc section, based on a series of papers published over the past 30 years (Amato et al. 2007; Barker et al. 1994; Behn & Kelemen 2006; Burns 1983, 1985; Burns et al. 1991; Clift et al. 2005a,b; DeBari & Coleman 1989; DeBari & Greene 2011; DeBari & Sleep 1991; Greene et al. 2006; Hacker et al. 2008; Johnsen 2007; Kelemen & Behn 2015; Kelemen et al. 2004, 2015; Mehl et al. 2003; Newberry et al. 1986; Plafker et al. 1989; Rioux 2006; Rioux et al. 2007, 2010; Trop et al. 2005). This Jurassic arc terrane is exposed from the Tonsina region, north of Valdez, Alaska, through the northern Chugach and southern Talkeetna Mountains to Palmer, Alaska, north of Anchorage, along the Kenai Peninsula south of Anchorage, and along the Alaska Peninsula westward to the vicinity of Katmai volcano (**Figure 2**). Interbedded volcanic and volcanoclastic rocks extend to a thickness of 5 to 9 km depth. These have variable compositions, ranging from basalt to rhyolite. The most common lava type is basalt, but the large range of intermediate to felsic lavas and the generally intermediate volcanoclastic compositions bring the average Talkeetna volcanic rock composition to 59.3 wt% SiO₂ and Mg# 0.49 (lavas: 57.9 wt% SiO₂, Mg# 0.49; volcanoclastic and pyroclastic: 63.2 wt% SiO₂, Mg# 0.47).¹ [For comparison, global average arc lava compositions from the compilation of Kelemen et al. (2004) are as follows: all: 56.3 wt% SiO₂, Mg# 0.47; oceanic: 55.7 wt% SiO₂, Mg# 0.48; continental: 56.9 wt% SiO₂, Mg# 0.47.]

The Talkeetna lava section is intruded by mafic to felsic plutonic rocks, with complex intrusive relationships. Though pyroxene-bearing gabbro and hornblende gabbro plutons are found

¹The detailed data set related to this discussion is provided in the **Supplemental Materials** (follow the **Supplemental Materials** link in the online version of this article or at <http://www.annualreviews.org/>). The supplement also includes the 2σ standard deviation of the mean. As the variabilities are generally much smaller than the variation discussed in this review, we omit this information from the main text to preserve readability.

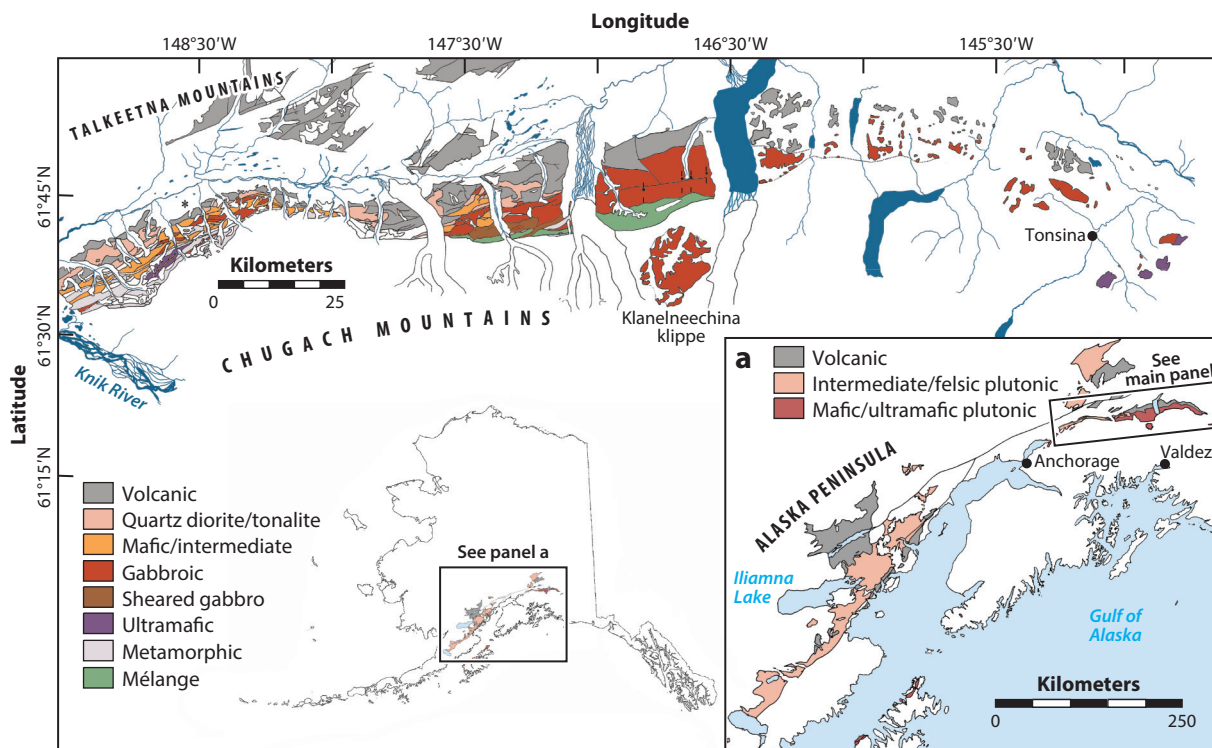


Figure 2

Simplified geological map of the Talkeetna arc. Figure modified with permission from Rioux et al. (2007, 2010).

at this crustal depth, and mafic enclaves in more felsic rocks are common, most of these mid-crustal plutons are hornblende tonalites and granodiorites, with an average of 65.1 wt% SiO_2 , and ~ 1 wt% K_2O , and Mg\# 0.42. In the western part of the Talkeetna arc section, on the Alaska Peninsula, these mid-crustal, intermediate-composition plutonic rocks dominate the exposed section (Johnsen 2007), over a strike length comparable to that of the iconic Sierra Nevada batholith in California. Both major and trace element characteristics of the average composition of mid-crustal plutonic rocks in the Talkeetna section are nearly identical to those of the average intermediate to felsic lavas in the section (**Figure 3**) (also see figure 20 in Kelemen et al. 2004, 2014), suggesting that the mid-crustal plutonic rocks do not necessarily represent cumulates but formed from magmas that crystallized 100% at depth.

At deeper crustal levels, the Talkeetna lower crust is characterized by hornblende magnetite gabbro, described extensively by Burns and coworkers (Burns 1983, Burns et al. 1991) and Greene et al. (2006). Though these rocks display modal layering in outcrop, and are intruded by a variety of other lithologies, in general the Talkeetna lower crust is homogeneous, with an average composition of 47.7 wt% SiO_2 and Mg\# 0.55. The gabbro, arises due to the high anorthite content in the plagioclase and the presence of 0–12% Fe-Ti oxides in Talkeetna gabbro. Greene et al. (2006) demonstrated that the gabbro are cumulates complementary to the average liquid line of descent of Talkeetna

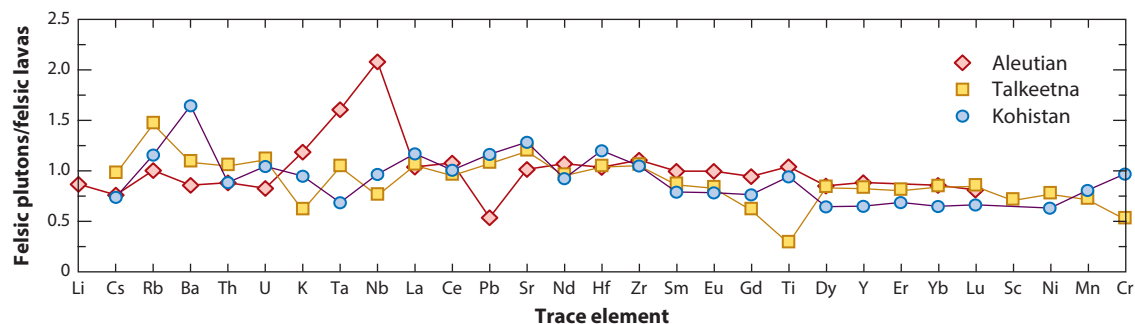


Figure 3

Average trace element ratio of felsic plutons to felsic lavas (≥ 54 wt% SiO_2). The trace element systematics of felsic lavas and plutons are essentially identical in Kohistan and Talkeetna. Aleutian plutons have apparently higher Nb and Ta concentrations compared with lavas, which might indicate the presence of cumulative Fe-Ti oxides. The Aleutian plutonic data set in our compilation, however, has limited Nb and Ta measurements.

lavas. The gabbro-norites, which are olivine and quartz free, formed in a narrow range of oxygen fugacity, 1 to 3 log units higher than that of the nickel-nickel oxide buffer (Behn & Kelemen 2006, Frost & Lindsley 1992).

An exception to the overall homogeneity of the Talkeetna lower crust is the presence of two-pyroxene, garnet quartz diorites in the Klanelneechina klippe, recording metamorphic conditions of $\sim 700^\circ\text{C}$ and 0.7 GPa and including bands and cross-cutting intrusions of garnet tonalite. Unlike metamorphic garnet granulites in the Moho depth exposures of the Tonsina region, Klanelneechina garnets are igneous (Kelemen et al. 2004, 2014). The average of eight Klanelneechina quartz diorites has a strikingly low Mg#, 0.32, with 49.2 wt% SiO_2 , whereas the average of three garnet tonalites has Mg# 0.25, with 72.0 wt% SiO_2 . The Klanelneechina quartz diorites, with their evolved compositions, may have been upper crustal arc lithologies—perhaps even volcanic rocks—that were gradually buried, enveloped in plutonic lower crust, metamorphosed, and ultimately partially melted within the growing arc edifice (see figure 26 in Kelemen et al. 2004, 2014). Alternatively, they could be buoyant lithologies underplated by relamination that were then differentiated by partial melting and melt extraction (Hacker et al. 2011).

The Tonsina region of the Talkeetna arc section has a series of exposures of the Moho, where arc plutonic and metamorphic rocks are in high-temperature contact with residual mantle peridotites. Much has been written about this region (Burns 1985; DeBari & Coleman 1989; Hacker et al. 2008; Kelemen et al. 2004, 2014; Mehl et al. 2003). Here we summarize a few salient points. Metamorphic phase equilibria for Tonsina samples record ~ 863 – 993°C and 0.8–1 GPa for garnet granulites, less precise values of 800– $1,000^\circ\text{C}$ and 0.9–1.2 GPa for hornblende gabbro-norite assemblages (with substantial sample-to-sample variability), and highly approximate conditions of $1,000^\circ\text{C}$ and 1 GPa for peridotites and gabbros that initially contained olivine plus plagioclase and now contain aluminous green spinel and two pyroxenes plus either olivine or plagioclase (Hacker et al. 2008). The igneous Talkeetna arc crust was ~ 40 km thick (DeBari & Coleman 1989, Hacker et al. 2008, Kelemen et al. 2015).

Near the base of the igneous crust, plagioclase-bearing lithologies are absent, and pyroxenites (websterite, orthopyroxenite, clinopyroxenite, and olivine clinopyroxenite) form a layer a few hundred meters thick between overlying gabbroic rocks and underlying residual mantle harzburgites and dunites. This thin crust-mantle transition in the Tonsina region is the only part of the Talkeetna section in which pyroxenes record Mg# between those in the residual mantle peridotites (0.92–0.90) and those in the lower crustal gabbro-norites (< 0.85) (Kelemen et al. 2015).

Petrologic models (Greene et al. 2006) and simple mass-balance considerations (see figure 25 in Kelemen et al. 2004, 2014) suggest that cumulates with Mg# between 0.85 and 0.9 should constitute more than 25% of the igneous section, rather than 1% as they do today. The pyroxenites are denser than the residual mantle peridotites (Behn & Kelemen 2006, Jull & Kelemen 2001). For this reason, it has been proposed that 25% to 35% of the original igneous mass of the Talkeetna arc was gravitationally unstable and foundered into the underlying mantle during or after arc magmatism (Greene et al. 2006; Jull & Kelemen 2001; Kelemen et al. 2004, 2014; Müntener et al. 2001). Metamorphic phase changes also formed garnet granulites and spinel-olivine pyroxenites that are denser than residual mantle peridotites (Behn & Kelemen 2006, Jull & Kelemen 2001). The protoliths were less dense gabbro-norites and olivine gabbros. Such densification processes could have caused gravitational instabilities (see Section 7).

Zircon geochronology indicates that the Talkeetna arc was active from ~210 to 160 Ma (Rioux et al. 2007, 2010), with younger plutonic rocks recording accretion with the Wrangellia terrane followed by magmatic episodes postdating accretion (Trop et al. 2005). A gradation from older ages in the south to younger ages in the north and northwest (Rioux et al. 2010) reveals that the locus of magmatic activity migrated northward (present-day coordinates), away from the subducting plate, perhaps due to subduction erosion (Clift et al. 2005b). This occurred over a period of ~50 Myr, similar to the northward migration of the active Aleutian arc.

The northward-dipping, lower crustal rocks exposed in the southern regions (e.g., Tonsina) are not the basement to the flat-lying volcanics and intermediate to felsic plutonic rocks in the northern regions (e.g., Talkeetna Mountains). If it is preserved, the lower crust beneath the northern region remains buried. Furthermore, there is only 15 km of structural thickness of the section extending from the Tonsina crust-mantle boundary outcrops (recording pressure ≥ 1 GPa) to the volcanics further north (DeBari & Sleep 1991, Hacker et al. 2008, Kelemen et al. 2015). Thus, accretion of the Talkeetna section and subsequent faulting resulted in substantial thinning of the section. Thermobarometry (Hacker et al. 2008) reveals that this thinning is not uniformly distributed over the section, resulting in substantial uncertainty about the composition of the middle crust (**Figure 4**).

Finally, a striking feature of the Talkeetna arc section is the general lack of older crust within the exposed arc section (Rioux et al. 2007, 2010). Exceptions are samples with inherited zircon in the suture with the Wrangellia terrane, in the northwestern Talkeetna Mountains. Older zircons are also found in a few metasedimentary roof pendants in the Alaska Peninsula batholith, perhaps indicating that this portion of the arc formed near a continental margin (Amato et al. 2007). Excluding the plutonic samples from the Talkeetna-Wrangellia suture, Nd and Sr isotope ratios for all but two samples of Talkeetna plutonic rocks (Greene et al. 2006; Rioux et al. 2007, 2010) and Nd isotopes for volcanic rocks (Clift et al. 2005a) lie within the compositional field for the Tonga arc (away from the Samoan hotspot).

We were unable to identify any remnants of older oceanic crust that might have hosted the arc section. Perhaps the prearc basement was removed by extension (e.g., Karig 1971). Large amphibolite lenses within the middle and lower crust do not represent older oceanic crust into which the arc was emplaced. Instead, they are light rare earth element-enriched andesites with Nb and Ta depletions, typical of arc magmas.

2.2. Kohistan Arc Crustal Section, Northern Pakistan

The Kohistan arc (**Figure 5**) forms a coherent tectonic block within the Himalayan belt and exposes a complete crustal arc section (Bard 1983, Jagoutz & Schmidt 2012, Tahirkheli 1979). In the north, unmetamorphosed sediments and volcanic rocks are exposed (Bignold et al. 2006, Petterson & Treloar 2004), whereas in the south, pressures reached ~1.5–1.8 GPa at the contact

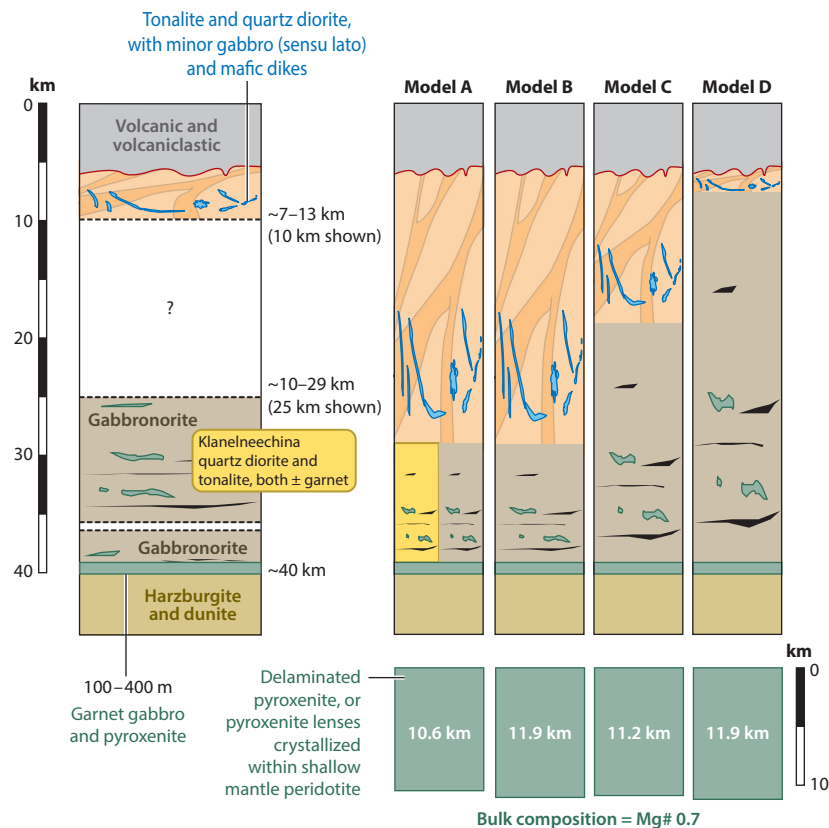


Figure 4

Simplified stratigraphic column of the Talkeetna arc section. (*Left*) The preserved rock types and their respective thicknesses. (*Right*) Four hypothetical columns where the preservation gap in the middle crust is systematically filled with more mafic compositions from A to D. Figure modified with permission from Kelemen et al. (2015).

between igneous arc crust and residual mantle (Garrido et al. 2007; Jan et al. 1989; Khan et al. 1993, 1989; Miller & Christensen 1994; Miller et al. 1991; Ringuette et al. 1999). Large-scale faulting related to, for example, the Himalayan collision is largely absent (Coward et al. 1982, 1986; Searle et al. 1999).

The volcanic units on top of the Kohistan arc are ~4–6 km thick and range from basalt to rhyolite (Bignold et al. 2006, Petterson & Treloar 2004, Petterson et al. 1991). Lavas are dominated by more mafic basaltic-andesitic compositions, yet felsic units, dominantly volcaniclastic, occur throughout and become especially volumetrically important in the Ladakh area (Clift et al. 2002), the western extension of the Kohistan arc. The average composition of the Kohistan volcanic rocks is 56.8 wt% SiO₂ and Mg# 0.58 (Jagoutz & Schmidt 2012), remarkably similar to average volcanic rocks in the Talkeetna section.²

²The detailed data set related to this discussion is provided as an electronic supplement associated with the paper by Jagoutz & Schmidt (2012). This supplement also includes the 2σ standard deviation of the mean. As the uncertainties are generally much smaller than the variation discussed in this review, we omit this information from the main text to preserve readability.

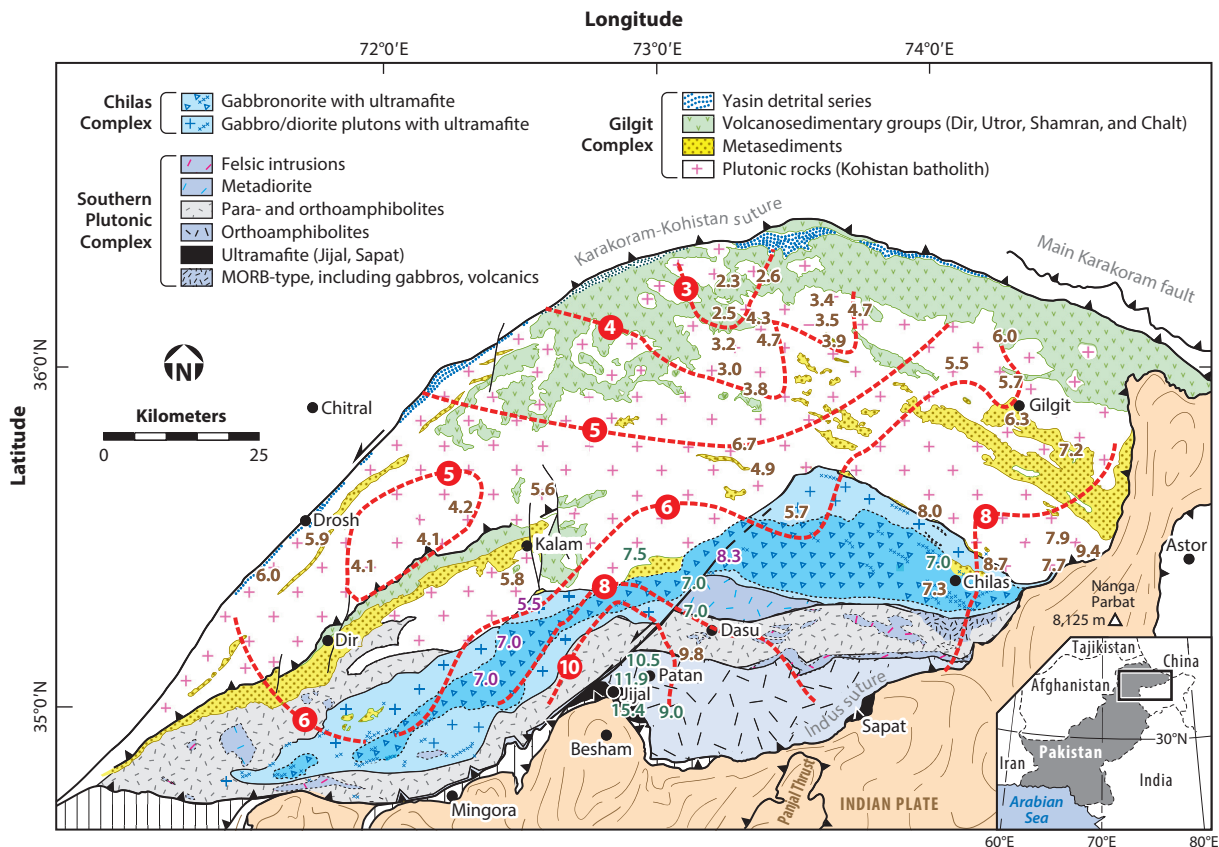


Figure 5

Simplified geological map of the Kohistan arc. Numbers indicate pressure in kilobars constrained by Al-in-hornblende barometry (brown) or by net transfer reactions involving garnet (green) or pyroxene-plagioclase-quartz (purple). The isobars (dashed red lines; associated numbers in red circles are in kilobars) illustrate the exhumation level of the Kohistan arc constrained by geostatistical modeling. Figure modified with permission from Jagoutz (2014). Abbreviation: MORB, mid-ocean ridge basalt.

The Kohistan volcanic section is deposited on top of, and intruded by, granitoids of the ~26-km-thick Kohistan batholith (Figure 5) (Jagoutz et al. 2013). The batholith ranges in composition from rare gabbro through (quartz) diorite, tonalite, granodiorite, and granite (Petterson & Windley 1985, 1991). Peraluminous leucogranites generally postdate the Himalayan collision and are not related to subduction zone processes (Bouilhol et al. 2013), so they are excluded from this review. Throughout the batholith, no systematic change of rock composition with depth is observed (Jagoutz et al. 2013). Most granitoids are hornblende and, to a lesser extent, biotite bearing, with magmatic epidote at pressures greater than ~0.45 GPa. Pyroxene-bearing granitoids are rare (Jagoutz et al. 2013). The average composition of the batholith is 64.6 wt% SiO₂ and Mg# 0.48 (Jagoutz & Schmidt 2012).

Toward the south, the Kohistan batholith is intruded by and intrudes the Chilas Complex, a large mafic-ultramafic intrusion (Jagoutz et al. 2007). The Chilas Complex is dominated by gabbro-norite and diorite associated with tabular bodies (~10 km long) of ultramafic units (dunite, pyroxenite, troctolite) (Jagoutz et al. 2006; Jan et al. 1992; Khan et al. 1989, 1993). Despite the local presence of magmatic layering, the mafic sequence of the Chilas Complex is surprisingly

homogeneous and has an estimated bulk composition of 53.1 wt% SiO₂ and Mg# 0.58. The ultramafic rocks of the Chilas Complex average 43.7 wt% SiO₂ and Mg# 0.82 (Jagoutz et al. 2006, Jagoutz & Schmidt 2012).

To the south, the Chilas Complex intrudes the Southern Plutonic Complex (SPC), a variable sequence of ultramafic to felsic plutonic and metamorphic rocks that make up the lowermost Kohistan arc crust (Burg et al. 2005; Dhuime et al. 2007, 2009; Garrido et al. 2006). The SPC is characterized by originally horizontal layers and sills of plutonic rocks (Jagoutz 2014). Minor volumes of amphibolite formed from metamorphosed volcanic units are preserved at the top of the SPC (Treloar et al. 1990, 1996). SPC mineral assemblages record 0.7 GPa at the top of the sequence and ~1.5–1.8 GPa at the base (Jagoutz et al. 2013, Ringuette et al. 1999, Yamamoto & Yoshino 1998, Yoshino & Okudaira 2004, Yoshino et al. 1998), roughly consistent with the structural thickness of the section. With increasing crustal depth, SPC plutonic rocks become more mafic (Jagoutz 2014, Jagoutz & Schmidt 2012). Mafic rocks in the Chilas Complex and SPC formed along two distinct liquid lines of descent from primitive, basaltic parental magmas: Chilas involved relatively dry crystal fractionation and production of predominantly gabbroic cumulates, and SPC formed via crystallization of a more water-rich magma, producing ultramafic cumulates (Jagoutz et al. 2011).

U-Pb zircon geochronology indicates that the Kohistan arc was active from at least ~120 Ma to the India-Kohistan arc collision at ~50 Ma (Bouilhol et al. 2013). The Kohistan batholith records arc magmatic activity from 120 to 50 Ma, whereas the Chilas Complex intruded at ~85 Ma (Schaltegger et al. 2002, Zeitler 1985) during incipient arc rifting (Burg et al. 2006). The SPC was formed from ~120 to 85 Ma (Dhuime et al. 2007, Schaltegger et al. 2002) and exhumed during arc extension (Burg et al. 2006). After 85 Ma, volumetrically minor felsic dikes intruded the SPC (Yamamoto et al. 2005).

Paleomagnetic data (Khan et al. 2009, Zaman & Torii 1999) are consistent with the hypothesis that the Kohistan arc was intraoceanic (Bard 1983, Tahirkheli 1979). Yet, the thickness of the Kohistan batholith resembles that of the Sierra Nevada batholith, which formed in a continental arc. Seismic data from active oceanic arcs do not show evidence for such thick batholiths (see the detailed discussion on seismic characteristics in Section 6.2), so that thick batholiths are thought to be characteristic of continental arcs. However, despite an extensive search, no old continental basement has been identified in the arc. No rock units are older than late Cretaceous, and none of the thousands of analyzed zircons are older than late Jurassic. In contrast, postcollisional leucogranites have abundant inherited zircons with Proterozoic and Mesozoic U-Pb ages derived from the colliding Eurasian and Indian crust (Bouilhol et al. 2013). Isotopically, the Kohistan arc is slightly more enriched than the Talkeetna arc, perhaps due to the presence of an enriched, Indian mid-ocean ridge basalt (MORB)-type component in the Kohistan mantle source (Zhang et al. 2005) and/or the recycling of a subducted sediment component as in active western Pacific arcs. The enrichment of the Kohistan arc relative to an Indian Ocean mantle source is comparable to the enrichment of Izu-Bonin-Mariana and Tonga arc lavas relative to a depleted mantle source (Jagoutz & Schmidt 2012).

3. COMPARISON WITH OCEANIC LOWER CRUST

In this section of the article, we briefly compare the composition of plutonic rocks in the Talkeetna and Kohistan arc sections with the composition of plutonic rocks formed at oceanic spreading ridges and of MORB (**Figure 6**). These include average MORB (our values and those from Gale et al. 2013), complete crustal sections through the Wadi Tayin and Nakhl massifs of the Oman ophiolite (Garrido et al. 2001, MacLeod & Yaouancq 2000, Peucker-Ehrenbrink et al. 2012,

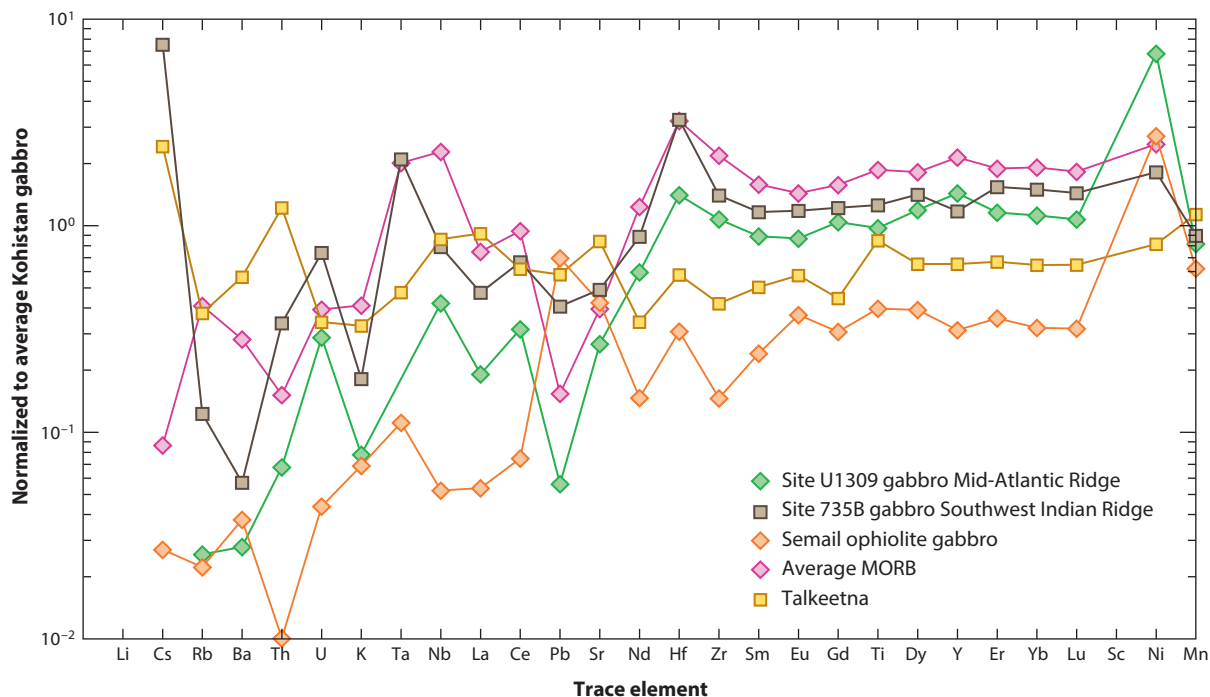


Figure 6

Trace element diagram normalized to average gabbros from Kohistan compared with gabbros from Talkeetna, oceanic crust [Ocean Drilling Program Site 735B (Dick et al. 2002) and Integrated Ocean Drilling Program Site U1309 (Godard et al. 2009)], and the Oman (Semail) ophiolite (Garrido et al. 2001, MacLeod & Yaouancq 2000, Peucker-Ehrenbrink et al. 2012, Yaouancq & MacLeod 2000; J.A. VanTongeren, P.B. Kelemen & K. Hanghøj, unpublished data). Abbreviation: MORB, mid-ocean ridge basalt.

Yaouancq & MacLeod 2000; J.A. VanTongeren, P.B. Kelemen & K. Hanghøj, unpublished data), the extensively sampled but incomplete 1.5-km gabbro section from Ocean Drilling Program (ODP) Hole 735B near the Southwest Indian Ocean Ridge (complete data set and review in Dick et al. 2002), and the extensively sampled but incomplete 1.8-km gabbro section from Integrated Ocean Drilling Program (IODP) Site U1309 near the Mid-Atlantic Ridge (Godard et al. 2009).

The average composition of Hole 735B gabbros is almost identical to an average, primitive MORB composition (Dick et al. 2002, Hart et al. 1999). Primitive cumulates at 735B are balanced by evolved ferrogabbros and tonalites, so the entire section approximates a 100% crystallized liquid. Thus, the 735B section is not complementary to evolved lavas on the nearby seafloor, which require a reservoir of primitive cumulates somewhere else.

Compared with all three of (a) average MORB, (b) U1309 gabbros, and (c) 735B gabbros (**Figure 6**), the Talkeetna and Kohistan lower crustal gabbro(norite)s are depleted in almost all compatible trace elements, and show striking, arc-like trace element patterns with relatively enriched light ion lithophile elements plus Pb and Sr; substantially depleted Nb, Ta, Zr, and Hf; and subdued heavy rare earth element concentrations, about three times lower than in MORB. Small enrichments of Eu and Ti in the average Talkeetna gabbro(norite), relative to MORB, reflect large enrichments of these elements relative to middle and heavy rare earth elements in primitive Talkeetna cumulates, due to uptake of Eu in cumulate plagioclase and Ti in cumulate Fe-Ti oxides.

Compared with cumulate gabbros from Oman, Talkeetna and Kohistan lower crustal lithologies are more light rare earth element enriched and have higher Al_2O_3 due to the high anorthite content in arc plagioclase, but the trace element patterns for the two suites are otherwise very similar. The fact that Oman gabbros are similar to Talkeetna gabbro-norites, which in turn have arc-like trace element characteristics when compared with MORB, provides one more piece of evidence supporting the hypothesis that the crust of the Oman ophiolite formed from arc-like primitive melts (e.g., Alabaster et al. 1982, MacLeod et al. 2013, Pearce et al. 1981).

4. COMPARISON WITH EXPOSED FRAGMENTS OF ARC LOWER CRUST

In addition to the complete or near-complete exposure of arc crust sections in Kohistan and Talkeetna, numerous incomplete arc sections are recognized. Deeper portions of arc crust are exposed in the Dariv and Hantashir Ranges of Mongolia (Bucholz et al. 2014, Zonenshain & Kuzmin 1978). Middle to lower crust of a continental arc is exposed in the Famatinian arc (DeBari 1994; Ducea et al. 2010; Otamendi et al. 2009, 2012). The southern Sierra Nevada batholith exposes mid- to lower crustal plutons and metasedimentary host rocks (Dodge et al. 1988; Domenick et al. 1983; Ducea & Saleeby 1996; Lee et al. 2006, 2007; Sisson et al. 1996). Similarly, the exposed Peninsular Ranges batholith formed at depths up to 20 km (Gastil 1975; Gromet & Silver 1987; Lee et al. 2006, 2007; Silver & Chappell 1988). Kelemen & Ghiorso (1986) reviewed the occurrence of ultramafic to mafic and ultramafic to felsic, mid-crustal, zoned plutonic complexes associated with arc batholiths worldwide. The intermediate to felsic plutonic rocks in these suites are generally calc-alkaline. These plutonic complexes are relatively small; similar bodies have been found in both Talkeetna and Kohistan, especially in the Chilas Complex of the Kohistan section (Jagoutz et al. 2006), where they constitute a small proportion of the mid-crustal suite. **Figure 7** presents major element data for several of these localities, compared with Talkeetna and Kohistan. We defer discussion of these data to Section 5.

By and large, we avoid the daunting task of compiling and analyzing data from continental arc batholiths. In so doing, we avoid the controversial procedure of discerning mantle contributions in plutons with a large component derived from partial melting or assimilation of preexisting continental crust or continentally derived sediments.

5. COMPARISON WITH MODERN INTRAOCEANIC ARCS

This article focuses mainly on the composition of plutonic rocks in the middle and lower crust of oceanic arcs. These are generally not well exposed in active intraoceanic arcs. Well-known suites of cumulate xenoliths have been recovered from several volcanoes in the Lesser Antilles (Arculus & Wills 1980, Kiddle et al. 2010, Parkinson et al. 2003, Tollan et al. 2012) and in the Aleutians (Conrad & Kay 1984, Conrad et al. 1983, DeBari et al. 1987, Yogodzinski & Kelemen 2007) and from Agrigan in the Mariana arc (Stern 1979). These samples are generally similar to those in the Talkeetna and Kohistan sections, for example in containing variable, sometimes substantial amounts of igneous hornblende and Fe-Ti oxides in rocks with high Mg# and high anorthite contents in plagioclase. In contrast, in gabbroic rocks from oceanic crust, both hornblende and Fe-Ti oxides are found only in evolved plutonic rocks, with low Mg# and sodic plagioclase.

Several intermediate to felsic plutonic complexes in southwest Japan and Komahashi-Daini Seamount were interpreted as exposures of mid-crustal plutonic rocks from the oceanic Izu-Bonin arc, uplifted during collision between Japan and the island arc (Haraguchi et al. 2003, Kawate 1996, Kawate & Arima 1998, Saito et al. 2007). However, more recent work has demonstrated that these

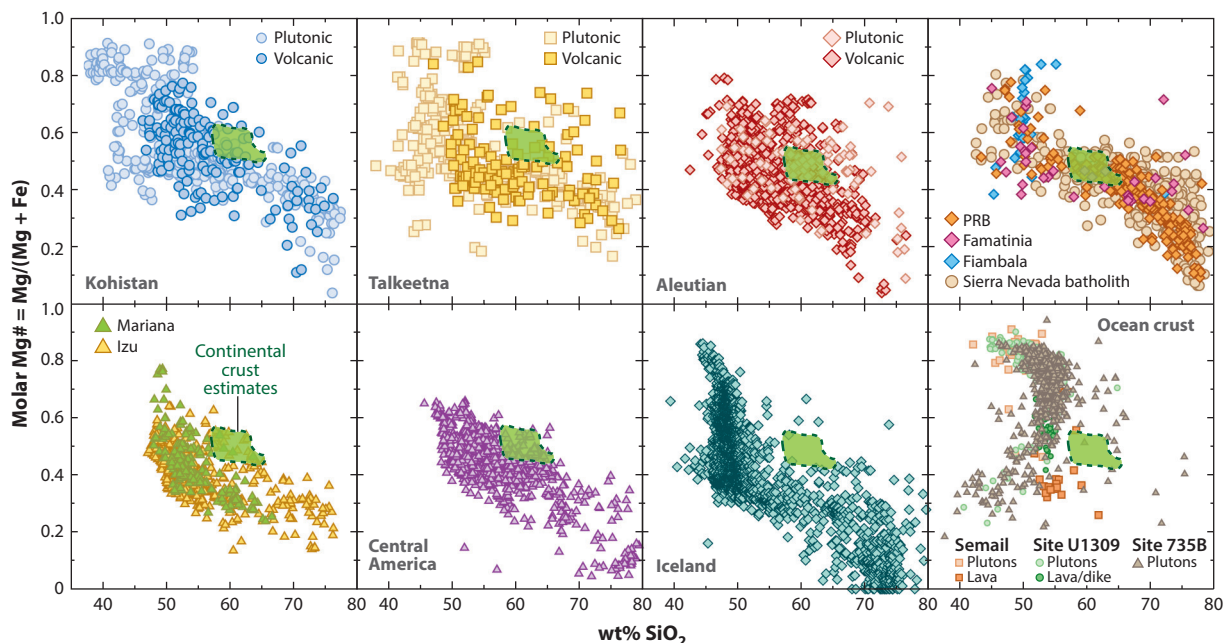


Figure 7

Relationship between SiO_2 and molar Mg\# [$\text{Mg}/(\text{Mg} + \text{Fe})$] for exposed volcanic and plutonic rocks from arc sections and active island arcs. For comparison, volcanic rocks from Iceland are also shown. Bulk continental crust estimates (*light green fields bounded by dark green dashed lines*) are based on the compilations of Rudnick & Gao (2004, 2014) and Hacker et al. (2011). Only a few arcs show magmatic differentiation that produces rock compositions that resemble bulk continental crust. Most arcs and Iceland have a differentiation path with too low an Mg\# at a given level of SiO_2 content to produce bulk continental crust. The tholeiitic trend observed in the oceanic crust cannot produce continental crust compositions. Data compiled from GEOROC (<http://georoc.mpch-mainz.gwdg.de/georoc/>). Abbreviation: PRB, Peninsular Ranges batholith.

intrusions are young, intrude the Honshu arc crust, and are related to the collision event rather than to arc magmatism (Tamura et al. 2010, Tani et al. 2011).

The Aleutian arc is unique among active intraoceanic arcs for its abundant exposures of mid-crustal plutonic rocks. The suite ranges from gabbro to granite; hornblende quartz diorite and granodiorite predominate. On the basis of limited geochemical data, we find that—as for mid-crustal rocks in the Talkeetna arc section—Aleutian intermediate to felsic plutons have liquid-like compositions (**Figure 3**). Unlike those of Talkeetna and Kohistan, Aleutian plutons are enriched in Th, U, K, La, and Ce compared with average lavas from the same islands. Aleutian plutons are also more strongly calc-alkaline than nearby lavas, with higher SiO_2 at a given Mg\# (figures 4 and 5 in Kelemen et al. 2003b). The plutons also have isotope ratios different from nearby lavas and similar to strongly calc-alkaline lavas in the western part of the arc (Cai et al. 2015), with high Nd and Hf isotope ratios and low Sr and Pb ratios.

The difference between plutons and lavas likely arises from the different viscosities of these two magma series, with the higher- SiO_2 (and, probably, higher- H_2O) magmas becoming highly viscous and stalling in the mid-crust, while the lower- SiO_2 , lower- H_2O , lower-viscosity basalts erupted freely (Kay et al. 1990, Kelemen et al. 2003b). This raises questions about whether primitive, erupted lavas are representative of the composition of the net magmatic flux from the mantle into arc crust, and emphasizes the need for continuing, complementary studies of plutonic suites in both active and accreted, ancient arcs.

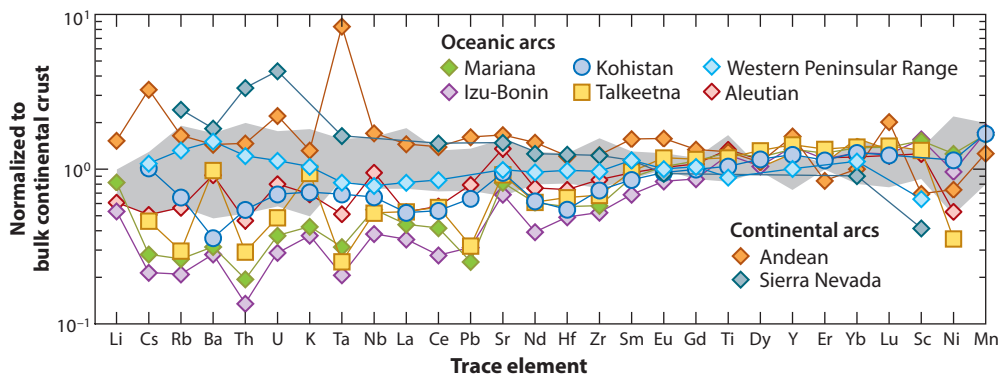


Figure 8

Continental crust-normalized trace element diagram of averaged volcanic and plutonic rocks from active arcs. The gray field outlines the estimates for average continental crust compositions. Continental margins [e.g., Andean, after GEOROC data, 2012 (<http://georoc.mpch-mainz.gwdg.de/georoc/>); Sierra Nevada, after Sisson et al. 1996] have significantly higher incompatible trace element concentrations compared with oceanic margins. The bulk continental crust estimates plot between the incompatible trace element concentrations of continental and oceanic margins, implying that continental crust is formed in both settings.

As shown by Kelemen and coworkers (Kelemen & Behn 2015; Kelemen et al. 2003b, 2004, 2014) and Gazel et al. (2015), both Aleutian lavas and plutons are more similar to continental crust than any other intraoceanic arc. Specifically, Aleutian arc rocks have highly enriched incompatible trace elements, unlike most oceanic arcs. This is true despite the fact that Aleutian lavas extend to the most isotopically depleted arc magma compositions worldwide (Kelemen & Behn 2015; Kelemen et al. 2004, 2014), with the smallest amount of recycled, old continentally derived components. The reasons for this phenomenon remain uncertain, but may include substantial input of partial melts derived from arc volcanics and plutonic rocks carried to mantle depth during subduction erosion, or from subducting oceanic crust (Kay 1978; Kelemen et al. 2003b; Yogodzinski et al. 1994, 1995; Yogodzinski & Kelemen 2000, 2007).

Generally, lavas and plutons in continental arcs have higher incompatible trace element concentrations than continental crust, whereas oceanic arcs have lower concentrations (**Figure 8**). Mixing these two would produce a composition that lies in the range of proposed continental compositions. The question arises: Why do continental arcs have higher incompatible trace element concentrations? One contribution is assimilation of preexisting continental crust. However, some primitive, continental arc magmas that show little or no evidence of assimilation also have high incompatible element concentrations, higher on average than in oceanic arcs (Kelemen et al. 2004, 2014).

Continental arcs (e.g., Andean, Sierra Nevada) have high elevations, whereas in most oceanic arcs (e.g., Izu-Bonin), only a few volcanic islands reach above sea level. Accordingly, continental arcs have significantly higher erosion levels than oceanic margins (Draut & Clift 2013). We speculate that increased surface erosion and subduction of trench sediments in continental arcs contribute to the observed difference in incompatible element budget between continental and oceanic arcs. In this context, the Aleutian arc, with its extensive exposures of mid-crustal plutonic rocks, represents an intermediate case.

Different magmatic differentiation processes take place in different arcs, as illustrated in SiO_2 -versus-Mg# diagrams (**Figure 7**). For comparison, we have also plotted volcanic rock compositions from Iceland [compiled from GEOROC data, 2012 (<http://georoc.mpch-mainz.gwdg.de/georoc/>)], and both plutons and lavas from mid-ocean ridges and the Oman ophiolite (data sources

cited in Section 3). Many arcs have relatively low Mg# (~ 0.3 – 0.5) at 55–65 wt% SiO₂ compared with estimated bulk continental crust (Mg# 0.50–0.60) (**Figure 7**). This difference is most pronounced for Iceland but is also evident in lavas from the Izu-Bonin, Mariana, Central America, Kohistan, and Talkeetna arcs. Continental crust could be produced in such arcs via mixing between felsic and mafic components. In contrast, lavas and plutonic rocks from the Aleutians and plutonic rocks from the Sierra Nevada and Peninsular Ranges batholiths with SiO₂ of 55–65 wt% have Mg# ~ 0.4 – 0.6 , within the range of bulk continental crust. Separation of these upper and mid-crustal lithologies from mafic lower crust could produce continental crust. Mechanisms for refining of arc crust to produce continental crust are discussed further in Section 7.

6. BULK COMPOSITION AND STRUCTURE OF ARC CRUST

Constraints on the bulk composition of arc crust can be obtained from inferences based on erupted lavas, from geophysical data [typically, seismic P and S wave velocity (V_P and V_S), sometimes combined with gravity and heat flow], and from direct observation of arc crustal sections. Also, lava series can be analyzed to infer the nature and proportions of minerals that crystallized from parental magmas to produce evolved compositions in order to identify likely compositions of arc cumulates. However, (*a*) lavas from modern, emergent volcanoes may not be representative of the time-averaged magma input; (*b*) there are melt-like plutonic rocks (not cumulates) in arc middle crust; (*c*) delamination may have removed dense cumulates from the base of arc crust; and (*d*) relamination may have added buoyant lithologies to the base of arc crust.

6.1. Field-Based Geochemical Estimates

Geological and geochemical studies of exposed arc sections potentially provide the best-constrained estimates of arc crust composition. However, arc crustal sections exhibit lateral variability, along and across strike. Also, tectonic processes may have produced gaps or repetition in the record of composition versus depth. Further, due to folding and/or tilting, even a continuous exposure—with all depths represented—may correspond to a diagonal rather than a vertical section through the crust.

Previous estimates for the bulk composition of both the Kohistan and Talkeetna arc crust (DeBari & Sleep 1991, Miller & Christensen 1994) assumed that the proportions of lithologies along arc-perpendicular transects were representative of their proportions in arc crust. In the case of the eastern Talkeetna transect, DeBari & Sleep (1991) noted that the structural thickness of the section (15–20 km) was about half of the thickness estimated from thermobarometry, and they attributed this to homogeneous thinning. These studies derived a mafic bulk composition (51 wt% SiO₂) for both the Kohistan and Talkeetna arcs. Greene et al. (2006) used a similar approach, but included a petrologic model of the average liquid line of descent to constrain the likely proportions of cumulate plutonic rocks. They too found that Talkeetna data are consistent with a range of basaltic bulk crust compositions with 48–51 wt% SiO₂.

Since then, Hacker et al. (2008) and Jagoutz & Schmidt (2012) have presented comprehensive thermobarometric results for the two arc sections and used these to constrain the bulk compositions. In the Talkeetna section, as noted in Section 2.1, thermobarometric data reveal that there is a gap in the exposures. Depending on the uncertainty bounds that are used, this gap extends from mid-crustal, felsic plutonic rocks emplaced at 5 to 9 km depth to lower crustal, mafic gabbro-norites at 17 to 24 km depth; the missing section is thus 8 to 19 km thick (**Figure 4**) (Behn & Kelemen 2006, Hacker et al. 2008, Kelemen et al. 2015). The inferred bulk composition of the Talkeetna crust depends on how one fills this gap.

Table 1 reports four different bulk compositions derived using different proportions of mafic gabbroanorites, Klanelneechina-type lower crustal quartz diorites, and mid-crustal felsic rocks to fill the major compositional gap, as discussed by Kelemen et al. (2015). The four alternatives have bulk compositions ranging from 61.7 to 50.4 wt% SiO_2 . The felsic estimates agree well with the geological map for Talkeetna, including the Alaska Peninsula batholith, in which $\sim 70\%$ of the exposed plutonic rocks are intermediate to felsic (**Figure 2**). However, geochemical similarities between the intraoceanic Talkeetna and Izu-Bonin-Mariana arcs, together with seismic data for Izu-Bonin discussed in Section 6.2.3, favor an intermediate composition, with about 56 wt% SiO_2 and Mg\# 0.52 (Kelemen et al. 2015).

Unlike in the case of the Talkeetna exposures, structural and barometric estimates for Kohistan agree and there are no evident gaps (Jagoutz & Schmidt 2012), with the exception that structural (5 km) and barometric (10 km) thicknesses of the lowermost garnet granulites disagree. To account for uncertainties, Jagoutz & Schmidt (2012) presented three different bulk compositions of the Kohistan crust. None include ultramafic rocks lying between the base of the plagioclase-bearing rocks and residual mantle peridotite. All are andesitic, with 57–59 wt% SiO_2 (**Table 1**; **Figure 9**). Some of these bulk compositions include extensive garnet granulites, with hornblende and pyroxenite lenses, near the base of the section. If the Kohistan section had not been accreted during the Himalayan continental collisions, these dense, mafic and ultramafic lithologies might eventually have delaminated. However, their presence or absence does not substantially affect the bulk silica content of the Kohistan section. Again, as for the Talkeetna section, these felsic, quantitative estimates are consistent with the geological map (**Figure 5**), on which felsic plutons constitute $\sim 50\%$ of the exposed plutonic rocks in the Kohistan arc section (Jagoutz & Schmidt 2012).

6.2. Seismic Properties of Arc Crust

In active arcs, outcrops are mainly limited to volcanic rocks. In order to constrain the deeper structure of active arcs, seismic data are essential. In the past decade, high-resolution studies of active arcs have revealed a wealth of new information on their seismic structure. Calvert (2011) and Hayes et al. (2013) recently reviewed seismic data on intraoceanic volcanic arcs and Costa Rica. Here we focus on data interpretation in terms of crustal lithology and in comparison with continental crust.

In this section, we first address two key questions pertinent to the interpretation of seismic sections for active arcs: What is the composition of the arc-mantle transition zone, where “crustal” P wave velocities gradually increase to “mantle” values? What is the significance of the higher seismic velocities observed in arc lower crust compared with continental crust?

6.2.1. Nature of the crust-mantle transition. In oceanic plates more than 20 Myr old, and in continental plates, the Moho is evident as a sharp seismic discontinuity, with V_P increasing from <7.4 km/s (above) to >7.7 km/s (below) over a vertical distance <2 km (**Figure 10**). Specifically, V_P at the base of oceanic crust increases from <7.3 km/s to an average of 7.95 km/s in the underlying mantle (data compilation by R.L. Carlson and P.B. Kelemen, figure F8 and related text in Shipboard Sci. Party 2004). Similarly, V_P at the base of continental crust increases over less than ~ 1 km from <7.4 km/s to an average of 8.1 km/s at $\sim 42 \pm 6$ km (**Figure 10**) (Christensen & Mooney 1995). In both tectonic settings, this discontinuity is interpreted as an abrupt transition from plagioclase-bearing igneous and metamorphic rocks in the crust to plagioclase-free, residual peridotites in the mantle.

In contrast, many arcs show a gradual increase in V_P with depth, from ~ 6.5 – 7.0 km/s at 10–20 km to >8 km/s at >50 km (**Figure 10**). Sharply defined discontinuities are rare or absent.

Table 1 Average values of lithological layers in the Talkeetna and Kohistan arc sections, together with estimated lower and bulk crust compositions and average compositions of buoyant lithologies in eclogite facies

Talkeetna				Kohistan										Density sorting: 700°C, 3 GPa, $\rho < 3377 \text{ kg/m}^3$				
Lavass	Mid-crustal plutons	Lower crustal gabbroic rocks	Bulk crust				Mid-crustal batholith	Lower crust			Bulk crust			1:1 mix buoyant Tal-keetna lavas + plutons	1:1 mix buoyant Kohistan lavas + plutons	1:1 mix buoyant Aleutian lavas + plutons		
			A	B	C	D		Lavas	1	2	3	1	2				3	
Mineral compositions (wt%)																		
SiO ₂	59.6	68.5	47.9	61.7	61.1	55.8	50.4	56.3	64.6	52.4	51.3	50.5	59.3	56.6	57.5	66.3	64.2	62.7
TiO ₂	0.86	0.50	0.66	0.63	0.59	0.64	0.68	0.74	0.62	0.74	0.79	0.84	0.68	0.73	0.73	0.85	0.54	0.66
Al ₂ O ₃	16.5	15.2	19.0	16.4	16.4	17.4	18.4	15.7	16.2	18.5	18.7	18.9	17.0	17.6	17.4	15.3	15.7	16.8
FeO ^T	7.78	4.06	9.94	6.38	6.33	7.84	9.39	7.74	4.66	8.09	9.20	9.97	6.26	7.44	7.34	5.02	4.61	5.19
MnO	0.19	0.11	0.18	0.15	0.14	0.16	0.18	0.17	0.10	0.15	0.17	0.19	0.13	0.15	0.15	0.13	0.12	0.12
MgO	3.57	1.67	7.78	3.43	3.85	5.42	7.03	6.04	2.38	6.56	6.43	6.03	4.32	4.93	4.37	2.69	2.94	2.69
CaO	6.30	4.66	12.53	6.91	7.22	9.23	11.31	7.70	5.03	10.14	10.44	10.92	7.21	8.26	7.94	4.15	4.77	5.48
Na ₂ O	3.82	4.38	1.82	3.64	3.54	2.88	2.20	3.25	3.92	2.74	2.50	2.28	3.42	3.08	3.12	3.69	3.90	4.05
K ₂ O	1.03	0.76	0.16	0.62	0.62	0.47	0.31	1.27	2.30	0.48	0.35	0.24	1.52	1.13	1.28	1.69	2.06	2.21
P ₂ O ₅	0.18	0.13	0.08	0.13	0.12	0.11	0.09	0.18	0.21	0.15	0.14	0.14	0.19	0.17	0.17	0.15	0.17	0.17
Mg# [molar Mg/(Mg + Fe)]																		
Mg#	0.45	0.42	0.58	0.49	0.52	0.55	0.57	0.58	0.48	0.59	0.55	0.52	0.55	0.54	0.51	0.49	0.53	0.48
Elemental compositions (ppm)																		
Rb	13.7	16.8	1.7	11.4	11.4	7.1	2.6	32.3	65.3	9.6	5.7	2.6	41.2	29.5	34.0	18.5	55.1	43.0
Ba	434	516	65	365	370	255	136	164	417	143	103	91	288	222	246	464	348	484
Th	1.27	1.72	0.07	1.17	1.16	0.74	0.31	3.07	6.16	1.21	0.71	0.27	4.00	2.88	3.22	1.83	5.24	4.60
U	0.67	0.88	0.04	0.60	0.60	0.39	0.17	0.90	1.82	0.17	0.10	0.07	1.11	0.79	0.95	0.83	1.18	1.96
K	8,271	8,397	1,120	6,202	6,210	4,353	2,436	10,575	19,130	3,987	2,882	1,993	12,618	9,380	10,625	14,038	17,112	18,265
Ta	0.15	0.17	0.03	0.14	0.13	0.09	0.05	5.28	7.45	2.57	1.84	1.03	0.34	0.26	0.29	3.10	6.21	11.45

(Continued)

Nb	2.41	2.41	0.40	2.03	1.81	1.30	0.77	0.48	0.47	0.11	0.09	0.06	5.41	4.15	4.36	0.22	0.48	0.86
La	7.5	7.8	1.2	6.1	5.8	4.1	2.3	10.5	21.9	7.2	5.2	4.3	15.2	11.7	12.9	9.6	16.0	15.2
Ce	16.8	17.4	2.9	13.7	13.0	9.3	5.5	23.2	41.9	15.5	11.8	10.0	30.2	23.6	25.8	20.6	33.2	33.5
Pb	4.3	3.3	1.2	2.7	2.8	2.3	1.7	7.1	9.7	3.6	2.8	1.8	7.1	5.7	5.9	4.0	7.8	8.0
Pr	2.4	2.4	0.5	1.9	1.8	1.3	0.8	5.5	4.6	1.8	1.4	1.4	3.6	2.9	3.2	2.8	4.2	4.5
Sr	248	228	300	249	251	269	288	304	459	342	310	275	399	364	362	261	338	493
Nd	11.6	11.5	2.6	9.4	8.9	6.6	4.3	12.4	17.8	9.0	7.5	6.9	14.0	11.6	12.4	12.9	14.5	18.5
Zr	84	108	11	80	76	51	25	96	161	52	39	30	113	88	96	117	134	160
Hf	2.61	3.38	0.39	2.47	2.38	1.61	0.82	2.03	3.56	1.12	0.86	0.56	2.49	1.93	2.07	3.19	3.13	4.44
Sm	3.7	3.7	1.0	3.0	2.9	2.2	1.5	3.3	3.8	2.1	1.9	2.0	3.1	2.7	3.0	3.8	3.4	4.3
Eu	1.10	0.97	0.47	0.90	0.84	0.71	0.58	1.05	1.00	0.82	0.80	0.83	0.93	0.89	0.93	1.08	0.97	1.08
Gd	4.3	4.3	1.4	3.6	3.4	2.6	1.9	3.7	3.5	2.7	2.6	2.5	3.2	3.0	3.1	3.7	3.5	4.3
Ti	4.448	3.417	3.188	3.797	3.481	3.425	3.367	4.460	3.734	4.416	4.735	5.035	4.075	4.375	4.375	5.117	3.210	3.922
Tb	0.78	0.78	0.25	0.65	0.62	0.49	0.35	0.69	0.54	0.40	0.41	0.44	0.43	0.43	0.45	1.25	0.61	0.60
Dy	5.1	5.1	1.7	4.3	4.1	3.2	2.3	4.2	3.3	2.6	2.7	2.9	3.1	3.0	3.2	4.7	3.7	4.0
Ho	1.10	1.11	0.37	0.93	0.89	0.70	0.50	1.20	0.65	0.55	0.58	0.64	0.67	0.65	0.70	1.01	0.85	0.81
Er	3.1	3.2	1.0	2.6	2.5	2.0	1.4	2.4	1.9	1.5	1.6	1.8	1.8	1.8	1.9	2.9	2.1	2.5
Yb	3.0	3.1	0.9	2.5	2.4	1.9	1.3	2.4	1.9	1.5	1.6	1.8	1.8	1.8	1.9	2.9	2.2	2.3
Lu	0.47	0.51	0.15	0.42	0.40	0.31	0.21	0.37	0.29	0.23	0.25	0.28	0.28	0.27	0.29	0.46	0.33	0.42
Y	29	30	9	25	24	19	13	24	17	16	16	17	17	17	18	29	21	28

Data sources: Talkeema: Kelemen et al. (2001, 2011, 2015); Kohistan: Jagoutz & Schmidt (2012); density-sorted compositions: Kelemen & Behn (2015). Average values are tabulated; median values and full data sets are available on request from the authors.

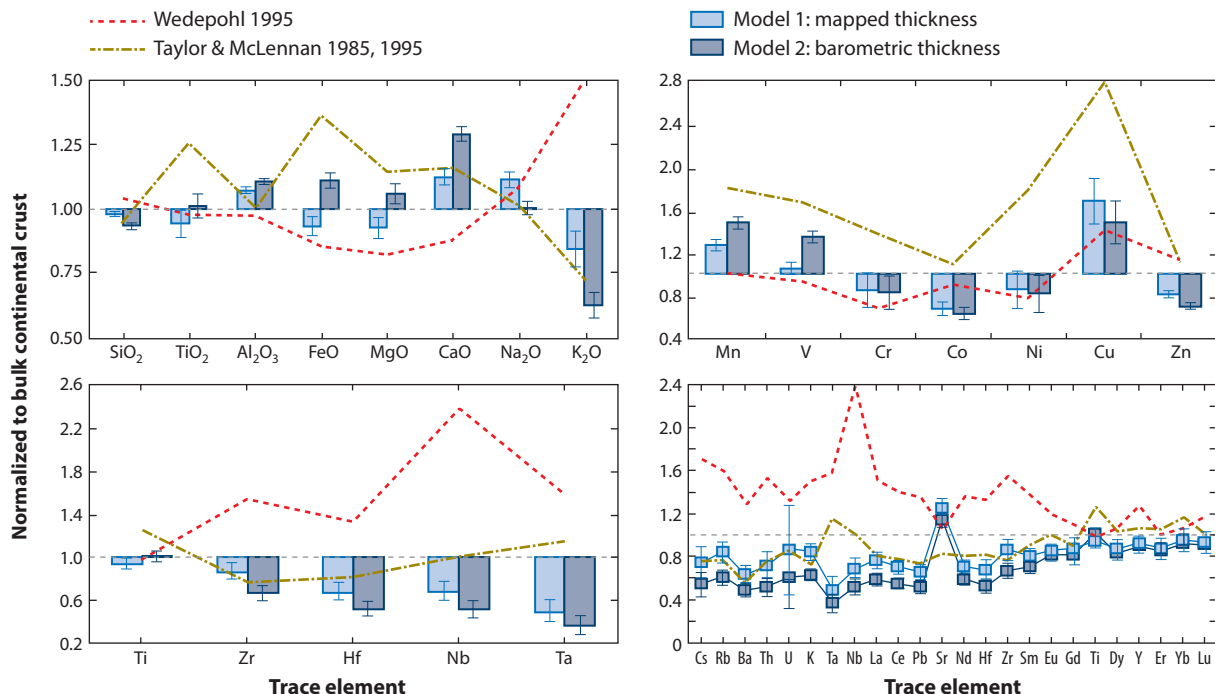


Figure 9

Bulk composition of the Kohistan arc for two different integration models compared with estimated bulk continental crust composition (Rudnick & Gao 2004, 2014). Both models yield an andesitic bulk composition for the Kohistan arc that is generally very similar to that of continental crust. Figure modified with permission from Jagoutz & Schmidt (2012).

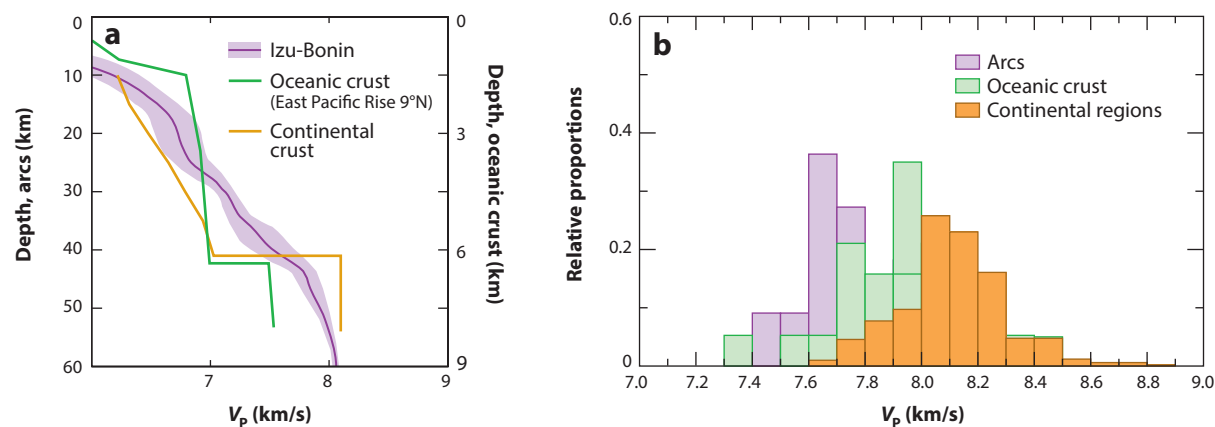


Figure 10

(a) One-dimensional seismic P wave velocity (V_p) profile of the Izu-Bonin crust (purple; Kodaira et al. 2007b), oceanic crust (green; scaled to the right axis after Vera et al. 1990), and bulk continental crust (orange; Christensen & Mooney 1995). (b) Histogram of sub-Moho velocities of arcs (purple), continental regions (orange), and oceanic crust (green). Whereas sub-Moho velocities in oceanic crust are similar to those in continents, sub-Moho velocities in arcs are significantly slower. Additional data sources: Calvert et al. (2008), Iwasaki et al. (1990, 1994), Janiszewski et al. (2013), Kodaira et al. (2007a,b), Kopp et al. (2011), Nakanishi et al. (2009), Shillington et al. (2004), Suyehiro et al. (1996), Takahashi et al. (2007, 2008).

Seismic velocities in rocks interpreted as lying beneath the Moho in arcs are, on average, ~ 0.3 – 0.5 km/s slower than sub-Moho velocities in continents. In contrast, velocities in lower crustal rocks in arcs, such as Izu-Bonin (reviews in Calvert 2011, Hayes et al. 2013), are generally ~ 0.2 – 0.5 km/s faster than in continents at the same depth (**Figure 10**). As a result of fast lower crustal velocities and slow sub-Moho velocities, the identification of a seismic discontinuity representing a Moho in arcs is difficult even in the best-studied regions (Izu-Bonin-Mariana and the Aleutians). Accordingly, estimates of arc crustal thickness are highly uncertain. For example, estimates of the depth to the Aleutian Moho range from 25–30 km (Holbrook et al. 1999) to 26–43 km (Janiszewski et al. 2013). Increasing evidence suggests that the base of the Aleutian and Izu-Bonin-Mariana crust is a $\gtrsim 5$ –15-km-thick transition zone rather than a sharp seismic discontinuity (Flügelner & Klempner 1999, Shillington et al. 2013, Takahashi et al. 2009, Tatsumi et al. 2008), with pyroxenites and even garnet-rich granulites below the “Moho.”

6.2.2. Sub-Moho seismic velocity structure. As discussed briefly above, sub-Moho lithologies with $V_P > 8$ km/s in continents and oceanic plates older than 20 Ma are generally interpreted as residual mantle peridotites. The possibility that they include abundant eclogite or garnet pyroxenite was debated in the middle of the twentieth century but has been largely abandoned owing to the paucity of eclogites in outcrops of the crust-mantle transition zone and in xenolith suites. Furthermore, as we show in Section 6.2.1, sub-Moho velocities in the continents are too high to allow for a significant proportion of typical pyroxenites. In contrast, “sub-Moho” velocities in arcs average 7.7 km/s (**Figure 10**). This leads to considerable ambiguity about the “sub-Moho” lithology in arcs.

Residual mantle peridotites beneath the Talkeetna arc lower crust are depleted harzburgites that record arc-parallel ductile flow (Mehl et al. 2003). Thermodynamic calculations using the *Perple_X* model (Connolly 1990, 2005) show that at 1 GPa, melt-free Talkeetna mantle harzburgite should have V_P of 8.0 km/s at 800°C and 7.9 km/s at 1,000°C, at the higher end of mantle V_P below arcs (**Figure 11**). In contrast, Tonsina garnet granulites, and gabbro-norites in garnet granulite facies, have an average V_P of ~ 7.3 km/s (Jagoutz & Behn 2013, Kelemen et al. 2015). Thus, the Tonsina Moho in its current configuration (after inferred delamination events) was a fairly abrupt lithological discontinuity. Once it cooled to $< 1,000^\circ\text{C}$, it would have also been an abrupt seismic discontinuity.

The concordant, interfingering, unfaulted contact between residual peridotites and gabbroic rocks recording equilibration temperatures $\sim 1,000^\circ\text{C}$ in Talkeetna, with just a few hundred meters of intervening pyroxenite, indicates that this is not a fault, and that in some arcs gabbroic lower crust overlies residual mantle peridotite, as in oceanic and continental crust. In these cases, low “sub-Moho” velocities might best be attributed to the presence of small melt fractions within peridotite, and to a steep temperature gradient, reaching $\sim 1,300^\circ\text{C}$ at 1.5 GPa (Kelemen et al. 2003a).

In contrast, garnet granulites, garnet hornblendites, and pyroxenites from Talkeetna (Behn & Kelemen 2006; Kelemen et al. 2004, 2014) and xenoliths from the Sierra Nevada (Lee et al. 2006, 2007) and Kohistan (Jagoutz & Behn 2013) have calculated V_P of 7.5–8.2 km/s in this depth and temperature range, with 89% of Talkeetna samples and 63% of Kohistan samples having V_P of < 7.8 km/s (**Figure 11**). Thus, “sub-Moho” lithologies in arcs with V_P of ~ 7.7 km/s could include abundant garnet granulite and pyroxenite, as proposed by Tatsumi et al. (2008) and Flügelner & Klempner (1999).

Recently, Shillington et al. (2013) found that the lowermost crust and uppermost mantle in the Aleutians—along a trench-parallel transect transitional between the forearc and the active arc—have V_P of 7.3–7.6 km/s and V_P/V_S of ~ 1.70 – 1.75 . This low V_P/V_S ratio may indicate that

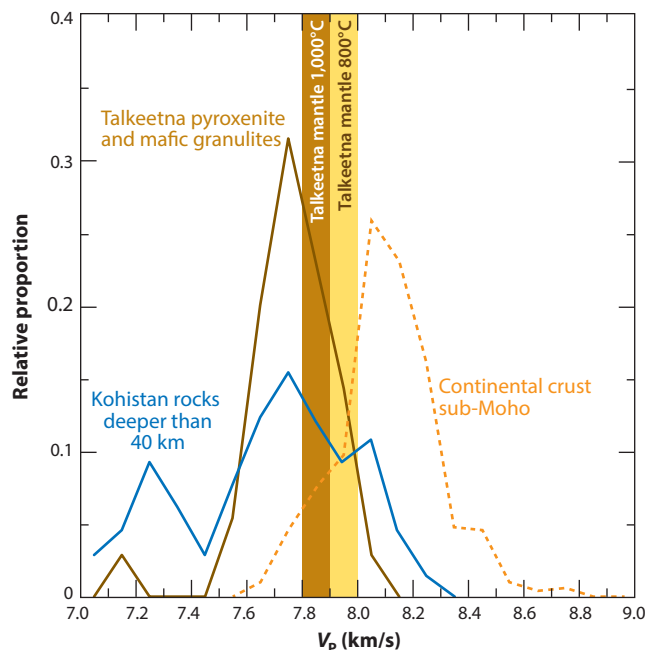


Figure 11

Histogram of calculated seismic P wave velocities (V_p) of rocks from Kohistan and Talkeetna (after Jagoutz & Behn 2013) compared with subcontinental Moho velocities (from Christensen & Mooney 1995).

the Aleutian lower crust is composed of mafic and ultramafic lithologies (e.g., pyroxenite, garnet granulite) together with α -quartz-bearing lithologies, perhaps resembling the two-pyroxene quartz diorites in Talkeetna discussed above. Importantly, at ~ 1 GPa, α -quartz is present only at $\lesssim 800^\circ\text{C}$. Improved seismic data for the lower crust directly beneath the active arc are needed to determine whether such low temperatures extend to this region.

Updating the pioneering efforts of Chroston & Simmons (1989) and Miller & Christensen (1994), Jagoutz & Behn (2013) calculated a one-dimensional seismic section for the Kohistan arc (**Figure 12**). Calculated V_p of the Kohistan lower crust is characterized by a gradual increase in V_p with depth, from 6.9–7.1 km/s at 30–35 km to ~ 8 km/s at 50–55 km. In this way, the Kohistan lower crust resembles lower crust in active arcs, characterized by the absence of a sharply defined Moho (Kodaira et al. 2007a,b; Shillington et al. 2004, 2013; Takahashi et al. 2008). Thus, if the Kohistan section is representative of active arcs, low- V_p sub-Moho lithologies correspond to mafic and ultramafic cumulate compositions (**Figure 11**).

As noted above, the pyroxenites and garnet granulites that constitute a large proportion of the lower crust in Kohistan are present only in a horizon a few hundred meters thick in Tonsina. Such a sharp compositional contrast in active arcs could be masked in seismic data for some regions by the presence of partial melt and/or temperatures $> 1,000^\circ\text{C}$ in the uppermost mantle. Elsewhere, as proposed for Kohistan by Jagoutz & Behn (2013), the smooth increase in V_p in active arcs may indicate the presence of thick layers of dense pyroxenite and garnet granulite that have not yet been removed by delamination. The presence of a sharp Moho in oceanic and continental plates may be the outcome of almost complete delamination of such dense cumulates and their replacement by upper mantle peridotite.

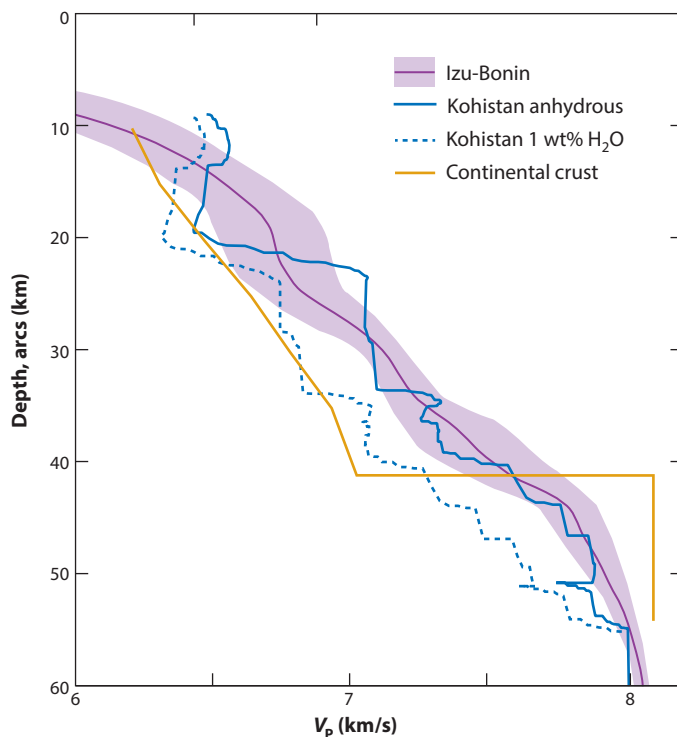


Figure 12

Seismic P wave velocities (V_P) in the Kohistan arc calculated along a 60-mW/m² geotherm assuming anhydrous conditions or 1 wt% H₂O (modified after Jagoutz & Behn 2013). The seismic velocities calculated for rocks from the uppermost 10–40 km of crust assuming 1 wt% H₂O are similar to those observed in continental crust, whereas the same rocks have seismic characteristics that resemble those of the Izu-Bonin arc when calculated assuming anhydrous conditions.

6.2.3. Supra-Moho seismic velocity structure. Seismic data may provide the most regionally comprehensive picture of the bulk composition of active and ancient arcs. The crustal seismic structure of arcs is highly variable within a given arc and between arcs. Thus, seismic data have been used to infer that both the Aleutian and Izu-Bonin-Mariana arc crust are basaltic (49–54 wt% SiO₂) (Flügel & Klemperer 1999; Holbrook et al. 1999; Kodaira et al. 2007a,b; Shillington et al. 2004; Tatsumi et al. 2008), whereas the Sierra Nevada batholith has low crustal V_P , indicating an intermediate to felsic bulk composition (Flügel et al. 2000). The Aleutian arc shows higher average V_P (6.8–7.5 km/s) at ~10–40 km depth (Flügel & Klemperer 1999; Holbrook et al. 1999; Shillington et al. 2004, 2013) compared with continental crust (6.3–7.0 km/s) over the same depth range. The Izu-Bonin arc has a broader range of V_P , 6.3–7.5 km/s (Kodaira et al. 2007a,b; Suyehiro et al. 1996; Takahashi et al. 2007, 2008; Tatsumi et al. 2008), overlapping both continental and Aleutian velocity profiles.

A calculated V_P profile for Kohistan, assuming anhydrous compositions (0 wt% H₂O), is about 0.3–0.5 km/s faster than the V_P profile of lower continental crust and essentially identical to that of the Izu-Bonin arc (with the exception of rocks at ~20 km depth) (Figure 12). Higher water contents stabilize phases with relatively low seismic velocities. Thus, a calculated V_P profile for Kohistan, assuming 1 wt% H₂O in the rocks, is similar to that of average continental crust at 10–40 km depth (Figure 12).

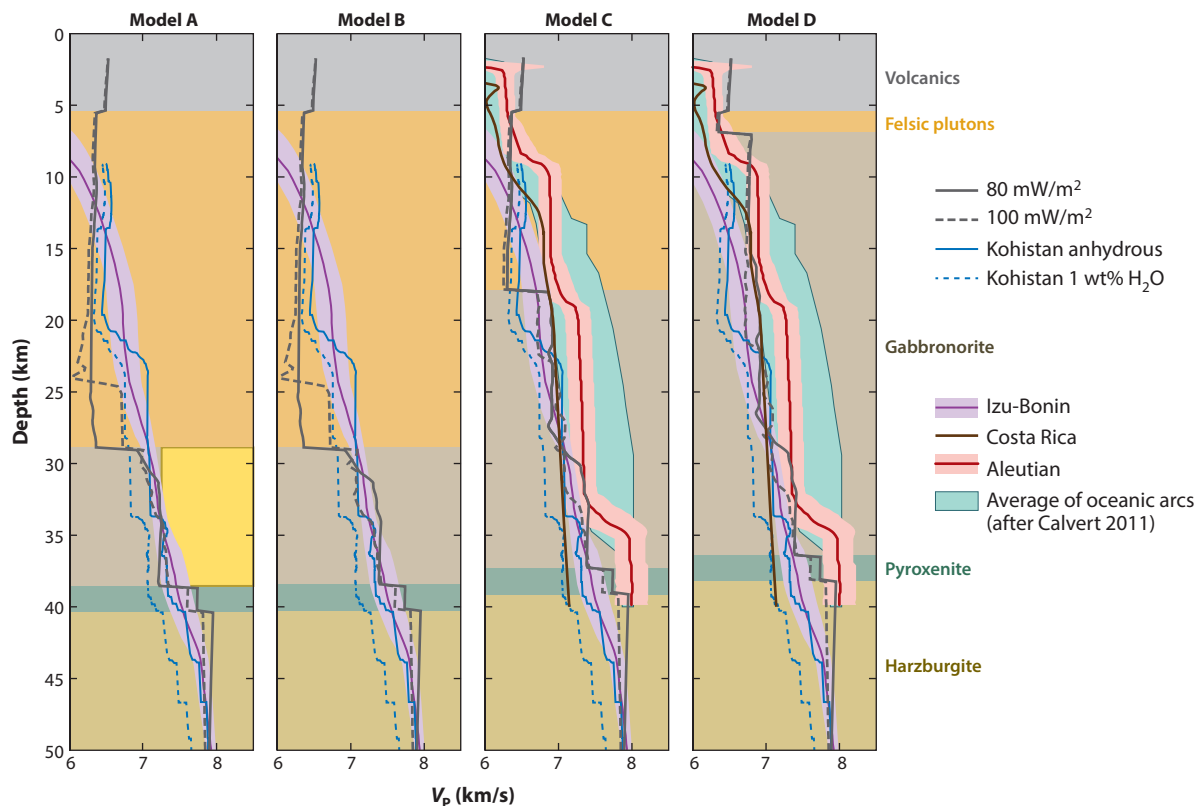


Figure 13

Calculated seismic sections for four possible compositions of Talkeetna lower crust, as illustrated in **Figure 4**. Calculations are for two different arc geotherms with surface heat flow of 80 mW/m² (solid gray lines; ~800°C at 30 km) and 100 mW/m² (dashed gray lines; ~1,000°C at 30 km). Seismic sections with the observed range and averages for the thicker parts of the Izu-Bonin arc (Kodaira et al. 2007a), the Aleutian arc (Shillington et al. 2004), and all volcanic arcs (Calvert 2011) are shown for comparison, as are calculated seismic sections for the Kohistan arc on a 60-mW/m² geotherm, with (slow) and without (fast) 1 wt% H₂O. Figure modified with permission from Kelemen et al. (2015).

Within the range of possible Talkeetna bulk compositions discussed in Section 6.1, intermediate and mafic compositions (56 and 50 wt% SiO₂, respectively; Kelemen et al. 2015), with 1 wt% H₂O, provide estimated V_P profiles (**Figure 13**) that most closely fit the average profile of V_P versus depth for the Aleutian arc from Atka to Unalaska Island (Shillington et al. 2004) and for the thicker part of the Izu arc (the region from 0 to 250 km along strike in figure 3 of Kodaira et al. 2007b). Possible felsic compositions for the Talkeetna crust (62 and 61 wt% SiO₂; Kelemen et al. 2015) have calculated middle and lower crustal V_P profiles that are systematically slower than the Aleutian and Izu seismic profiles (figure 3 of Kelemen et al. 2015), and similar to the Central Sierra Nevada profile P4 of Fliedner et al. (2000) with velocities of 6.0–6.4 km/s extending to ~30 km depth.

Based on the calculated seismic profiles for Kohistan and Talkeetna, discussed in the previous two paragraphs, some of the differences between the seismic characteristics of the uppermost 40 km between arcs and continental crust could be related to water content—for example, alteration during arc continent collision and/or subsequent metamorphic events—and/or to compositional

differences. Regardless of their specific differences, the Kohistan arc crust is known to be andesitic and the Izu-Bonin and Talkeetna arc crust could be andesitic. These compositions are buoyant relative to the mantle, so they are difficult to subduct and thus are additions to continental crust. However, the significantly higher seismic velocities observed, for example, in the Aleutian arc almost certainly indicate that some arc crust is significantly more mafic than continental crust.

7. TRANSFORMATION OF ARC CRUST TO CONTINENTAL CRUST

Continental crust, as well as lavas and intermediate to felsic plutonic rocks in some arcs, has a calc-alkaline composition defined by relatively high SiO_2 and alkali element concentrations and relatively low CaO at a given Mg# (Arculus 2003, Irvine & Baragar 1971, Miyashiro 1974). Typical calc-alkaline magmas are high-Mg# (>0.4) andesites and dacites with $\sim 55\text{--}65$ wt% SiO_2 . In contrast, lavas and compositionally similar plutonic rocks, with low SiO_2 and alkalis at a given Mg#, are often termed tholeiitic. Typical tholeiitic magmas are basalts with <53 wt% SiO_2 at Mg# 0.3–0.6. Whereas tholeiitic lavas are found at oceanic spreading ridges, ocean island volcanoes, and large igneous provinces as well as in arcs, calc-alkaline lavas and plutonic rocks are almost exclusively found in arcs.

7.1. Formation of Calc-Alkaline Andesites and Dacites

It is well established that tholeiitic magma series can be produced by crystal fractionation from primitive, mantle-derived basalts at low fugacities of oxygen ($f\text{O}_2$) and/or H_2O ($f\text{H}_2\text{O}$) (Grove & Baker 1984). In contrast, the origin of calc-alkaline lava series is less well understood, and is generally attributed to one of three general recipes (**Figure 14**):

1. fractionation of a primitive³ basaltic or picritic parent (Mg# >0.6), with high $f\text{O}_2$ and/or $f\text{H}_2\text{O}$, driving crystallization of abundant Fe-Ti oxides, garnet, and/or hornblende early in the crystallization sequence (e.g., Blatter et al. 2013, Gill 1981, Grove et al. 2003b) (**Figure 14a**);
2. mixing of highly evolved “granitic” liquids with high SiO_2 and low Fe and Mg, with primitive basaltic liquids whose high Fe and Mg contents lead to high Mg# in the mixtures (e.g., Anderson 1976, Sisson et al. 1996) (**Figure 14b**); or
3. fractionation from a primitive andesite rather than a primitive basalt (e.g., Grove et al. 2003b, Müntener et al. 2001) (**Figure 14c**).

In a variant to recipe 2, mechanical juxtaposition of unrelated felsic and mafic rocks could also produce a calc-alkaline crustal composition, without involving any calc-alkaline magmas. In this article, we do not discuss the relative merits of these three recipes, but we emphasize that all three recipes require subsequent modification to produce the intermediate bulk composition of continental crust (**Figure 14d**).

7.2. Geochemical Transformation

All estimates indicate that bulk continental crust has the composition of andesites and dacites with 57–67 wt% SiO_2 and Mg# 0.44–0.57 (estimates compiled by Hacker et al. 2011, 2015; Kelemen

³Note that we have assumed that most or all magmas passing from the mantle into arc crust are in Fe/Mg exchange equilibrium with mantle olivine and/or pyroxene with Mg# $\sim 0.89\text{--}0.92$. Partial melting of mafic eclogites and/or pyroxenites in the mantle—for example, metabasalts in subducting oceanic crust—is quite possible, even likely, but we consider that most such melts react and reach Fe/Mg equilibrium with residual mantle peridotite before reaching the base of arc crust.

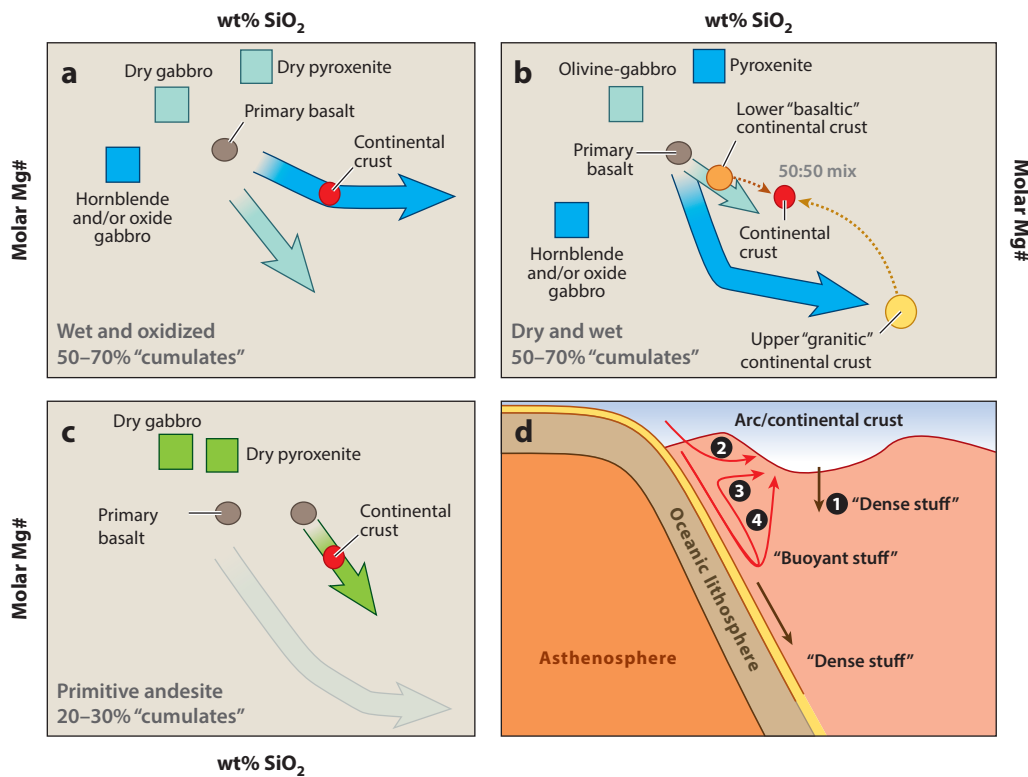


Figure 14

Schematic illustrations of different continental crust formation paths. (a) Certain fractionation paths result in rock compositions that resemble bulk continental crust compositions. Examples of such differentiation trends are observed in, for example, the Aleutians and the Sierra Nevada (see **Figure 7** for details). (b) Other arcs show a differentiation trend that has too low an Mg# at a given level of SiO₂ content to produce rock compositions akin to bulk continental crust. If these arcs contribute significantly to continental crustal growth, the continental bulk composition can be explained as (mathematical) mixing between a felsic and mafic end-member. Examples of such differentiation trends are found in the Kohistan, Talkeetna, Izu-Bonin-Mariana, and Central American arcs (see **Figure 7** for details). (c) Continental crust may be formed predominantly by high-Mg# andesite, in which case the andesitic bulk composition of the continental crust could be produced by differentiation. Examples of these kinds of melts are found in, for example, the Aleutians. Regardless of the preferred formation mechanism (panels a–c), a certain component must be removed from the system, as the composition of bulk continental crust is not in equilibrium with an upper mantle mineral assemblage. Panel d illustrates different density sorting mechanisms (1–4) that might result in the separation of the more felsic material that forms the continental crust from the more mafic material that complements the bulk continental crust to a primitive melt composition.

1995; Rudnick & Gao 2004, 2014). In contrast, magmas in Fe/Mg exchange equilibrium with mantle olivine and pyroxene (Mg# ~0.9) have Mg# >0.6. Thus, if most magmas that form arc crust are in Fe/Mg exchange equilibrium with the mantle, an additional mechanism is required to produce continental crust with lower Mg#.

It has been proposed that weathering processes may play a role in this transformation (e.g., Albarede & Michard 1986, Lee et al. 2008). Despite the geochemical importance of weathering throughout geological history, we doubt that weathering has been the primary factor converting mantle-derived magmatic crust to continental crust. Subaerial leaching of preexisting magmatic crust would preferentially remove K and Na compared with Mg and Fe, and would remove more Mg than Fe, at least at high *f*O₂ since ~2 Ga, providing a poor match for the alkali-rich,

high-Mg# composition of continental crust (Kelemen 1995). Oxidative seafloor weathering may have provided increased alkali contents and higher K/Na to the arc magmatic source since ~2 Ga (Jagoutz 2013, Rosing et al. 2006), but—given the similarity of Archean and post-Archean crustal compositions (Taylor & McLennan 1985, 1995; Weaver & Tarney 1984) and of Archean and post-Archean granulites (Hacker et al. 2015, Huang et al. 2013, Rudnick & Presper 1990)—this seems to have been a minor effect. However, mechanical and chemical erosion may remove subaerial lavas, exposing felsic plutonic rocks that are resistant to erosion. In arcs such as the Aleutians, more than half the lavas are basaltic whereas mid-crustal plutons are relatively felsic (reviews and averages in Kay et al. 1990, Kelemen & Behn 2015, Kelemen et al. 2003b). Even so, to transform arc crust into continental crust, an additional process must remove the mafic sediments as well as mafic lower crust. As a result, we do not discuss weathering further in this article.

7.3. Density Sorting

Most workers agree that, in order to make the transformation from mantle-derived magmatic crust to continental crust, density sorting must occur, via

1. delamination⁴ of dense lower crustal lithologies (Arndt & Goldstein 1989, Herzberg et al. 1983, Jagoutz & Behn 2013, Jull & Kelemen 2001, Kay & Kay 1991, Ringwood & Green 1966, Wernicke et al. 1996) (path ① in **Figure 14d**), either (a) during and immediately after arc magmatism (Jagoutz & Behn 2013; Jull & Kelemen 2001; Kelemen et al. 2004, 2014) or (b) during later tectonic events involving extensive metamorphism at garnet granulite- or eclogite-facies conditions, together with Moho temperatures >700°C (e.g., Saleeby et al. 2003); or
2. relamination of buoyant, subducting compositions (Hacker et al. 2011, Kelemen & Behn 2015) via (a) imbrication (e.g., Ducea et al. 2009, Grove et al. 2003a), involving incomplete subduction in which buoyant material never descends below the crust-mantle transition zone and instead is thrust into or just beneath the base of arc crust (path ② in **Figure 14d**), (b) ascent along a “subduction channel” (e.g., Cloos & Shreve 1988, Gerya et al. 2002, Warren et al. 2008, Whitney et al. 2009) (path ③ in **Figure 14d**), or (c) rise of diapirs through the mantle wedge (e.g., Behn et al. 2011; Chatterjee & Jagoutz 2015; Gerya & Yuen 2003; Kelemen et al. 2004, 2014; Little et al. 2011) (path ④ in **Figure 14d**).

An alternative to density sorting might be the preservation of arc cumulates with Mg# >>0.6 (e.g., wehrlite, pyroxenite, garnet granulite) below the continental Moho (where we use the term cumulate to indicate a rock formed by partial crystallization of a parental melt, followed by removal of the remaining melt). However, whereas the “mantle wedge” in arcs often has sub-Moho $V_P < 8$ km/s, continental upper mantle typically has sub-Moho $V_P > 8$ km/s, as discussed in Section 6.2.1. Whereas subarc mantle might contain abundant ultramafic cumulates with seismic velocities ~7.7 km/s, as discussed above, the continental upper mantle probably has relatively few. Thus, a role for density sorting in the transformation from arc to continental crust seems essential.

7.3.1. Relamination. Relamination occurs when buoyant lithologies are subducted into denser upper mantle and are then emplaced at the base of the crust. Relamination processes potentially exhibit substantial variability, as noted above. Subduction erosion (von Huene & Scholl 1991)

⁴For some, the term delamination implies transport of an intact, tabular layer of crust (or cold mantle) deeper into the upper mantle. For others, the terms delamination and foundering can be considered essentially synonymous, and include viscous, diapiric flow of dense lithologies into the underlying mantle. We use the term delamination in this second sense.

may commonly involve imbrication or underplating of buoyant material. Geodynamic calculations suggest that buoyant lithologies, with layer thicknesses in excess of ~ 100 m, will always undergo unstable, diapiric rise through denser peridotite once the temperature of both lithologies exceeds ~ 700 – 800°C (Behn et al. 2011, Jull & Kelemen 2001, Kelemen & Behn 2015, Miller & Behn 2012).

Evidence for relamination is provided by high-pressure (HP) and ultrahigh-pressure (UHP) metamorphic rocks, which were subducted to depths >40 km and >100 km, respectively, and then returned to the base of the crust (~ 35 km) prior to later exhumation (summaries in Hacker et al. 2011, Walsh & Hacker 2004). In most cases (U)HP terranes record nearly adiabatic decompression, inferred to result from ascent along a relatively cold “subduction channel,” but in some cases, exhumation pressure-temperature (P-T) paths are consistent with ascent through a hot mantle wedge (Chatterjee & Jagoutz 2015, Little et al. 2011). At even higher temperature, highly efficient recycling of geochemical sediment components into arc magmas (Behn et al. 2011) and the presence of gnospydite xenoliths derived from metasediments but recording mantle wedge P-T (Sharp et al. 1992) are consistent with buoyant, metasedimentary diapirs rising through the mantle wedge.

Distinctive peraluminous metasediments are common in lower continental crust (Hacker et al. 2011, 2015), perhaps as a result of relamination. This provides a minimum estimate of the proportion of metasediments in lower crust, because many volcanoclastic, forearc sediments are similar to intermediate igneous rocks (McLennan et al. 1990). During sediment subduction and subduction erosion, such sediments, plus lavas and intermediate to felsic plutons, may be thrust into or just below arc lower crust, as observed in metamorphic terranes (e.g., Ducea et al. 2009, Grove et al. 2003a) and inferred from seismic data (Bassett et al. 2010, Scherwath et al. 2010). Relamination of buoyant magmatic rocks may be common. Archean and post-Archean granulite terranes are dominated by felsic, quartzofeldspathic gneisses, which could have been relaminated as described above. A clear example is a remnant of jadeite granite in the Western Alps (Compagnoni & Maffeo 1973), which preserves HP mineral parageneses, within a larger mass of felsic rocks whose HP history was obliterated during retrograde metamorphism.

Kelemen & Behn (2015) noted that the trace element composition of lower continental crust—inferred from updated average compositions for continental granulite xenoliths and granulite terranes (Hacker et al. 2015, Huang et al. 2013)—is similar to that of bulk continental crust and very different from that of arc lower crust in the Kohistan and Talkeetna sections, even after the likely effects of delamination have been taken into account. In contrast, relamination of buoyant arc material—after it is subducted as trench sediment, via subduction erosion and/or during arc-arc and arc-continent collisions—provides a good explanation for the observed trace element composition of lower continental crust (**Table 1**).

7.3.2. Delamination and the formation of the continental Moho. Delamination could occur in active arcs or later, for example from the base of continental crust. Jull & Kelemen (2001) argued that delamination of dense lower crust, on geologically relevant timescales, is unlikely below $\sim 700^\circ\text{C}$ because the rate of diapiric flow becomes very small at low temperature. Thus, delamination occurs only where the base of the crust is unusually hot compared with continental interiors. This can happen in arcs, in overthickened crust rich in heat-producing elements, and during rifting. Delamination has been invoked as an important process in the evolution of both Talkeetna (as discussed in Section 2.1) and Kohistan (as discussed in this section). Both arc sections lack the volume of primitive cumulates ($\text{Mg\#} > 0.85$) required to explain the volume of more evolved cumulate pluton and lava compositions (Jagoutz & Schmidt 2013; figures 24 and 25 in

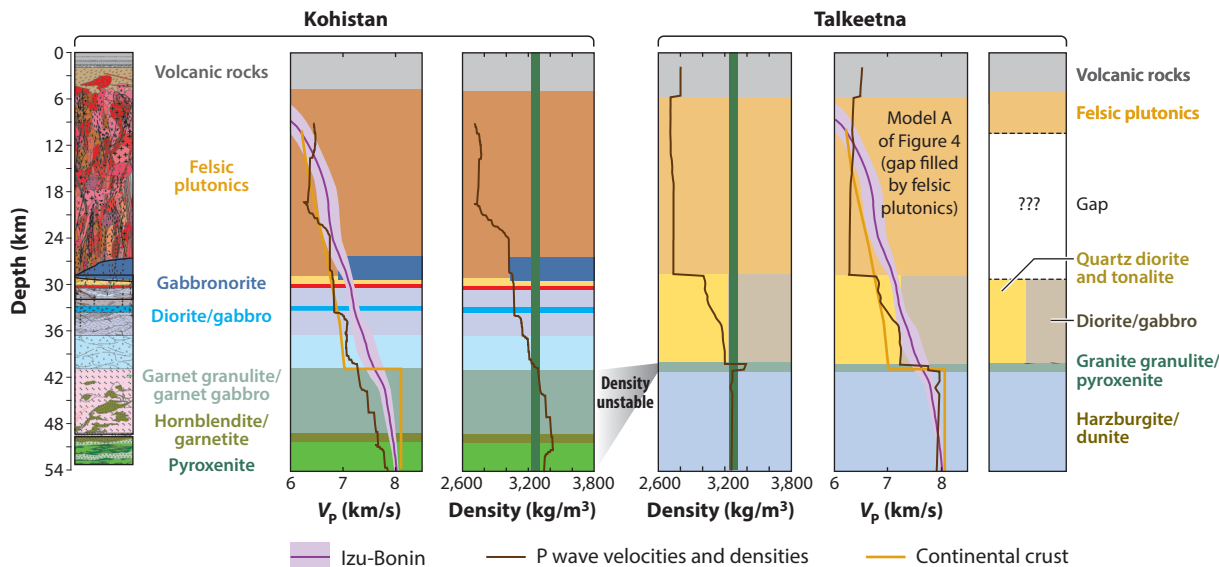


Figure 15

Schematic illustrations of the lithological, seismic, and density properties of the Kohistan and Talkeetna arc sections. Shown are simplified, schematic crustal columns and the calculated average seismic P wave velocities (V_p) and densities (dark brown lines) of the main crustal building blocks of the two arcs. Each dark green vertical band represents the density of peridotitic upper mantle at ~ 15 kbar. The reconstructed Kohistan section is seismically similar to the active Izu arc section, and the lower arc crust is denser than the underlying mantle at depths exceeding ~ 40 km. In contrast, the reconstructed Talkeetna section shows a jump in seismic velocities at the sharply defined crust-mantle transition, similar to that observed in continental regions. Density-unstable rocks are only preserved as relicts in Talkeetna, indicating that Talkeetna is density sorted. Figure modified with permission from Jagoutz & Behn (2013).

Kelemen et al. 2004, 2014), and this lack is best understood as the result of delamination of dense, primitive pyroxenite compositions.

Mafic garnet gabbro/granulites, hornblende/garnetites, and pyroxenites in the Kohistan and Talkeetna lower crust become density unstable at $\gtrsim 1.0$ – 1.2 GPa, which correlates well with the depth of the continental Moho (Jagoutz & Behn 2013, Jagoutz & Schmidt 2013, Behn & Kelemen 2006, Jull & Kelemen 2001, Müntener et al. 2001). Therefore, these lithologies had the potential to sink into the upper mantle. If the density-unstable layer is replaced by mantle peridotite, after cooling below $1,000^\circ\text{C}$ the resulting contact between remaining arc lower crust and peridotite will have an abrupt increase in seismic velocities, with the depth range and velocity contrast characteristic of the continental Moho (Figure 15).

7.3.2.1. Quantifying the timescales of delamination. The density difference between Kohistan and Talkeetna ultramafic cumulates and garnet granulites on the one hand and upper mantle peridotites on the other is $\Delta\rho = \rho_{\text{crust}} - \rho_{\text{mantle}} = 40$ – 280 kg/m^3 . Using these densities, magma flux rates of 215 – 290 $\text{km}^3/\text{km}/\text{Myr}$, and a temperature of 700°C to $1,100^\circ\text{C}$ for the underlying mantle, Jagoutz & Behn (2013) calculated that the periodicity of instability development ranged from <0.5 to ~ 5 Ma for unstable layers <1 to ~ 15 km thick (Figure 16). Based on the thermal conditions recorded at the base of the Kohistan (700 – 800°C) and Talkeetna (800 – $1,000^\circ\text{C}$) arcs, and on arc magma production rates (see Section 7.3.2.2), the model predicts layer thicknesses of

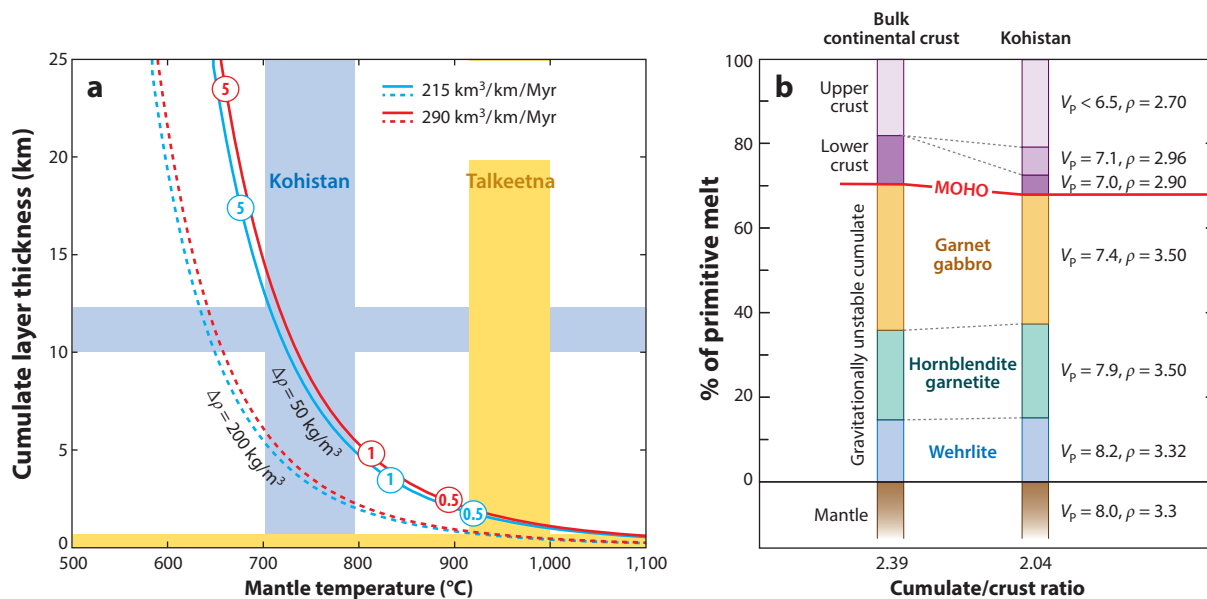


Figure 16

(a) Modeled thickness of the density-unstable layer at the base of arc crust (after Jagoutz & Behn 2013). The numbers in red and blue circles are times required to grow each layer in millions of years. The vertical bands indicate the approximate Moho temperature for the Talkeetna (yellow) and Kohistan (blue) arcs, and the corresponding horizontal bands indicate the preserved thickness of the density-unstable layer in the two arcs. (b) Proportions of different model calculations for the delaminated cumulates needed to balance primitive melt compositions to the Kohistan bulk crust and the bulk continental crust (Rudnick & Gao 2004), illustrating the relative masses of gravitationally unstable cumulates and arc crust. The calculations indicate that ~55–70% of the original melt mass is returned to the upper mantle as density-unstable cumulates in order to produce andesitic continental crust. V_p values are in km/s; ρ values are in kg/m³. Figure modified with permission from Jagoutz & Schmidt (2013).

~10–12 km for Kohistan and <1 km for Talkeetna, consistent with the observed thickness of the preserved dense layers (~12 km in Kohistan and ~100 m in Talkeetna).

7.3.2.2. Quantifying the rates of mass transport associated with delamination in arcs. Constraining the rates of mass transport in subduction zones and arcs is difficult. Whereas the amount of subducted oceanic crust is essentially equal to the amount of oceanic crust produced at ridges (~18–19 km³/yr), the rates of mass transport due to sediment subduction, arc magmatism, delamination, subduction erosion, and relamination are uncertain and depend on many assumptions (Jicha & Jagoutz 2015). In recent years, significant progress has been made in quantifying the rates related to surface erosion and subduction erosion (Clift & Vannucchi 2004, von Huene & Scholl 1991). Crust production rates have also been better constrained, though estimates still vary by a factor of five (Dimalanta et al. 2002, Jicha et al. 2006, Reymer & Schubert 1984). Frequently, the crustal production rate is assumed to be equal to the rate of magmatic transport into arc crust (Crisp 1984). However, this method for estimating the crustal production rate is correct only if there has been no significant delamination, subduction erosion, and/or relamination (Jicha & Jagoutz 2015).

Instead, some arc crust has a more evolved composition because of delamination (see Sections 2.1 and 7.3.2), and there is evidence for relamination (Section 7.3.1), though the

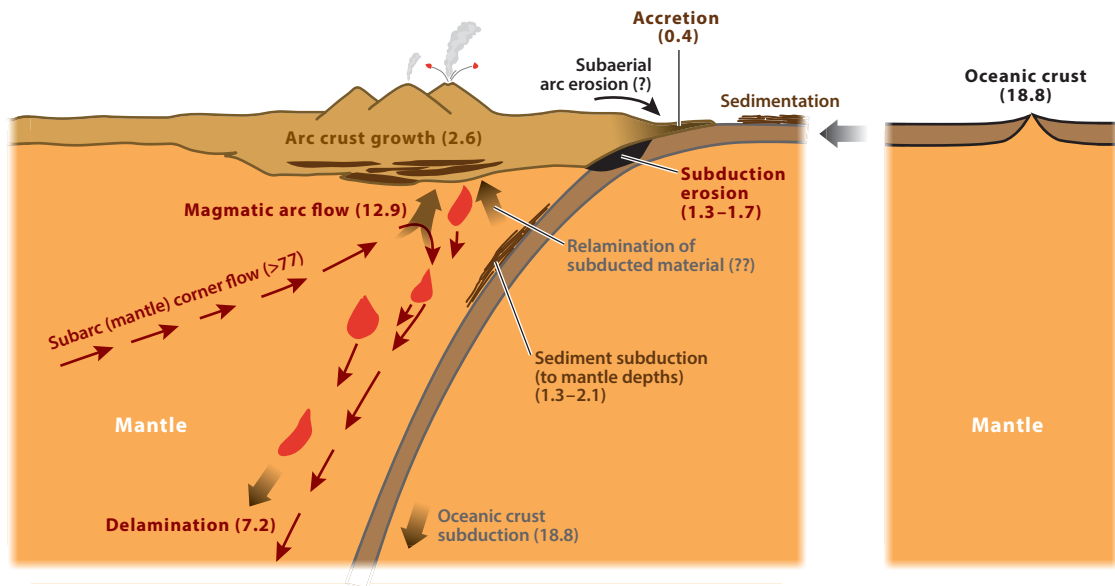


Figure 17

Mass fluxes (in km^3/yr) in a subduction zone, as constrained by Jagoutz & Schmidt (2013). The amount of material that is relaminated remains poorly constrained. Figure modified with permission from Jagoutz & Schmidt (2013).

relamination fluxes are not well constrained (Hacker et al. 2011). Thus, the arc crustal volume is produced by magmatic addition, minus the material removed by delamination and subduction erosion, plus the material added by relamination.

To constrain the arc magma production rate, the bulk compositions of remaining arc crust, density-unstable rocks, crust removed by subduction erosion, added buoyant rocks, and primitive arc melts need to be known, together with the duration of arc processes. Jagoutz & Schmidt (2013) calculated the Kohistan arc magma production rate; their results are summarized in **Figure 17**. If the arc had a basaltic parent magma, 60–70% of density-unstable material is needed to balance the current, andesitic bulk composition of the Kohistan arc (**Figure 16**) (Jagoutz & Schmidt 2013).

This result, which does not account for relamination, is in accord with more general estimates for the removal of ultramafic to mafic material required to produce continental crust from basaltic arc crust (Kelemen & Behn 2015, Lee et al. 2007, Plank 2005). Thus, for example, a compilation of experimental data yields 48–90% crystallization (with one experiment yielding 23%) to produce andesitic compositions similar to that of Kohistan crust from hydrous basalt, and 25–60% crystallization if the parental magma is a primitive andesite (Kelemen & Behn 2015). As the preserved volume of dense rocks ($\sim 20\%$) is not sufficient to balance the existing Kohistan arc crust, significant volumes of dense material must have been delaminated during arc activity. This suggests that the amount of material removed by delamination and/or subduction erosion in Kohistan was about two-thirds of the total arc magma production. Incorporating the crust production rate for Kohistan and some global estimates for subduction erosion, Jagoutz & Schmidt (2013) concluded that the arc magma production rate is about 11–14 km^3/yr (corresponding to 215–290 $\text{km}^3/\text{km}/\text{Myr}$), about two-thirds of the mid-ocean ridge magma production rate. Recently, Jicha & Jagoutz (2015) extended the approach of Jagoutz & Schmidt (2013), described above, to a

global compilation of active intraoceanic arcs. Their results indicate that global magma production rates vary between 152 and 220 km³/km/Myr for the Tonga-Kermadec and Izu arcs, respectively.

Such high magma production rates are in apparent conflict with constraints from heat flow data (from other regions) that indicate significantly lower magma production rates of 10–50 km³/km/Myr (Ingebritsen et al. 1989). Further, the high values for arc magma flux deduced by Jicha & Jagoutz (2015) appear to be inconsistent with rates of recycling of key components from subducting sediments in arc magmas. If arc magma production rates $\gtrsim 60$ km³/km/Myr are correct, the assumption that, for example, most of the Th in arc magmas is recycled from subducting sediments yields impossibly high recycling proportions: (Th concentration in primitive arc magmas \times arc magma flux) / (Th concentration in subducting sediment \times sediment subduction flux) > 1 (e.g., Behn et al. 2011, supplementary figure 3). This indicates that either estimates for arc magma flux greater than ~ 60 km³/km/Myr are too high or much of the recycled Th and other components are derived from subducting oceanic crust, not just from subducting sediment.

We are not sure how to resolve these apparent discrepancies. Thus, we feel that the apparent contradiction between different lines of evidence on arc magma fluxes presents an interesting problem for future resolution.

Delamination could have a significant effect on the isotopic evolution of the mantle (Jagoutz & Schmidt 2013, Lee et al. 2007, Tatsumi 2000, Tatsumi et al. 2008). The mass of delaminated material could be as much as 50% of the mass of subducted oceanic crust, and delaminated lithologies may host a significant proportion of some trace elements. For example, the Pb concentration of the delaminated material estimated for Kohistan and Talkeetna, ~ 2 –3 ppm, is 5 to 10 times higher than in average MORB (Gale et al. 2013), and U/Pb and Th/Pb in lower crustal gabbroic rocks are more than 20 times lower than in primitive mantle (McDonough & Sun 1995). On the one hand, as proposed by Lee et al. (2007) and by Jagoutz & Schmidt (2013), delaminated material has a low μ ($\mu = {}^{238}\text{U}/{}^{204}\text{Pb}$), of ~ 0.3 , which may help to explain the so-called Pb paradox (Allegre 1969), balancing the radiogenic composition of MORB and ocean island basalts (instead of or in addition to highly depleted peridotites; Kelemen et al. 2007, Malaviarachchi et al. 2008, Warren & Shirey 2012). On the other hand, Tatsumi (2000) estimated that the delaminated component from the Izu-Bonin-Mariana arc would evolve toward enriched mantle II Pb isotope characteristics intermediate between those of bulk Earth and the MORB source.

The realization that the mass of delaminated material could be $\sim 50\%$ of the mass of subducted oceanic crust opens many new and exciting scientific questions. For example, the delaminated material in Kohistan includes a significant proportion of hydrous minerals such as hornblende. As hornblende has an upper pressure stability limit of ~ 2 –3 GPa, amphibole in descending diapirs will break down and release H₂O, possibly triggering dehydration melting of the delaminating material and/or flux melting of the surrounding upper mantle, as previously proposed by Ringwood & Green (1966) and by Bédard (2006).

8. SUMMARY

8.1. Andesitic Arc Crust in Some Times and Places

For years it was thought that the bulk composition of all oceanic arcs was essentially basaltic. This assumption was based on seismic observations of active arcs and reconstruction of the Kohistan and Talkeetna exposed arc sections. However, high-resolution seismic data on the Izu-Bonin arc indicate the presence of volumetrically important amounts of felsic middle crust, so that the bulk crustal composition might be andesitic (Kodaira et al. 2007a,b; Suyehiro et al. 1996; Takahashi et al. 2007, 2008; Tatsumi et al. 2008). Similarly, as discussed in Section 6.1, reevaluation of the

Kohistan section reveals that it is andesitic, with a major element composition within the range of estimated bulk continental crust (Jagoutz & Schmidt 2012). For the Talkeetna crust, recent P-T estimates indicate significant gaps in the preservation of the upper plutonic arc crust, making its bulk composition model dependent, but possibilities include andesitic compositions with up to 62 wt% SiO₂.

8.2. No Vestige of a Beginning

The Kohistan and Talkeetna arcs formed in an intraoceanic setting, accommodated by extension of preexisting crust. We have been surprised by the difficulty of locating prearc host rocks, into which these plutonic rocks were emplaced. For the Kohistan arc prior to its collision with the Indian subcontinent, and for the Talkeetna arc south of its suture zone with the older Wrangellia terrane, only a few zircon analyses reveal even a hint of inheritance from prearc sediments. Similarly, we have been unsuccessful in identifying preexisting oceanic crust among metavolcanics and gabbros. Isotope data for both sections indicate derivation from a depleted mantle source. Although Kohistan and Talkeetna may include components recycled from subducting sediments, such a component is just as subdued as in the Tonga and Izu-Bonin-Mariana arcs, so that the Kohistan and Talkeetna sections represent almost entirely juvenile, igneous crust, derived mainly from partial melting of the mantle and—perhaps—mantle-derived MORB in subduction zones.

8.3. Remarkably Consistent Crustal Thickness

When considering the seismic “crust,” composed mainly of plagioclase-bearing plutonic and metamorphic rocks with $V_p \lesssim 7.5$ km/s, the Kohistan, Talkeetna, and Aleutian sections have strikingly similar thicknesses, of about 40 km (Jagoutz & Schmidt 2013, Janiszewski et al. 2013, Kelemen et al. 2015), as may also be the case for the thicker parts of the Izu-Bonin arc (see **Figure 12**, which shows data from Kodaira et al. 2007b). This may be attributed to both (a) the increase in seismic velocity and density due to the formation of cumulate ultramafic rocks plus igneous and/or metamorphic garnet below these depths and (b) foundering of dense lithologies into underlying mantle peridotite when the temperature exceeds ~ 700 – 800°C at these depths (see Section 7.3.2).

9. RECIPES FOR CONTINENTAL CRUST

As outlined in Section 1, the continental crust paradox relates to the apparent discrepancy between the basaltic net flux from the mantle into arc crust (<52 wt% SiO₂, Mg# >0.65) and the andesitic to dacitic continental crust (56–66 wt% SiO₂, Mg# 0.43–0.55). This apparent paradox is generally resolved either by modifying the composition of the net flux or through density sorting mechanisms. As reviewed above, some propose that the net magmatic flux from the mantle to the crust is (or has been) andesitic in some places (or at some times in the past). This may well be true. However, as noted above—if most arc magmas entering the crust are in Fe/Mg exchange equilibrium with residual mantle peridotite—some transformation is nevertheless required to reduce the crustal Mg# from more than 0.65 to less than 0.55.

Another modification of flux is the hypothesis that garnet granulites and/or ultramafic lithologies remain below the continental Moho and above residual mantle peridotite; bulk continental crust including these lithologies might have Mg# >0.65 . However, we believe that this is unlikely, owing to the observation that V_p is consistently >8.1 km/s in the subcontinental mantle.

Thus, density sorting via gravitational instabilities—delamination of dense material and/or relamination of buoyant material—seems to be an essential process in transforming arc crust to continental crust.

10. CONCLUSION

The simple processes of arc subduction and density sorting outlined in this article could have operated virtually unchanged over much of Earth history to produce continental crust. Although it is uncertain whether subduction-related magmatic processes have continued throughout Earth history, it is increasingly clear that the main characteristics of subduction magmatism—hydrous, fluxed melting of the mantle, with recycling of material descending from the surface of a wet planet—has continued in some form since 4.2 Ga (Grimes et al. 2007; Hopkins et al. 2008, 2010). Given the range of estimated global arc crustal production rates (2.0 to 3.8 km³/yr; Clift et al. 2009) and the total volume of continental crust ($\sim 6.0 \times 10^9$ km³), all continental crust, and a similar volume of subducted, dense residues ($\sim 2.4 \times 10^9$ to 10^{10} km³), could have been produced by arc subduction and density sorting over the course of Earth history. As a result, there is no obvious requirement for additional mechanisms of continental genesis and growth.

Several aspects of the process described here may have been somewhat different in the past. Low f_{O_2} might have rendered crystallization of Fe-Ti oxide minerals, to form high-Mg# andesites from basalts, less likely. Or primitive and high-Mg# andesites and dacites with enriched trace element concentrations may have been more common as a result of extensive partial melting of mafic volcanics as they subducted or foundered into a hotter mantle (Drummond & Defant 1990, Martin 1986, Rapp & Watson 1995, Rapp et al. 1991). The mantle wedge above Archean subduction zones may have been composed of highly depleted, residual dunite (Bernstein et al. 2007), reacting with ascending melts but contributing a smaller mantle component to arc magmatism than in modern arcs (Kelemen et al. 1998).

Obviously, in addition to arc subduction and density sorting, many other processes have contributed to the development of continental crust. However, the end-member hypotheses offered here have the advantage of simplicity, fit compositional and dynamical constraints, and provide quantitative benchmarks against which other explanations can be compared. Additionally, the two end-member models of density sorting (delamination and relamination) can be tested in the future by better constraining the bulk composition of lower continental crust.

DISCLOSURE STATEMENT

The authors are not aware of any affiliations, memberships, funding, or financial holdings that might be perceived as affecting the objectivity of this review.

ACKNOWLEDGMENTS

We thank Tom Sisson, Shuichi Kodaira, Gene Yogodzinski, Merry Cai, Andrew Greene, and Sue DeBari for providing background data sets and figure templates, and Brad Hacker and Mark Behn for insightful advice and ongoing collaborations that provided the basis for much of this article. P.B.K.'s efforts in completing this article were supported in part by National Science Foundation (NSF) grants OCE-1144759 and EAR-1049905. O.J.'s work was supported by NSF grants EAR-0910644 and EAR-1322032.

LITERATURE CITED

- Alabaster T, Pearce JA, Malpas J. 1982. The volcanic stratigraphy and petrogenesis of the Oman ophiolite complex. *Contrib. Mineral. Petrol.* 81:168–83
- Albarede F, Michard A. 1986. Transfer of continental Mg, S, O and U to the mantle through hydrothermal alteration of the oceanic crust. *Chem. Geol.* 57:1–15

- Allegre CJ. 1969. Comportement des systèmes U-Th-Pb dans le manteau supérieur et modèle d'évolution de ce dernier au cours des temps géologiques. *Earth Planet. Sci. Lett.* 5:261–69
- Amato JM, Rioux ME, Kelemen PB, Gehrels GE, Clift PD, et al. 2007. U-Pb geochronology of volcanic rocks from the Jurassic Talkeetna formation and detrital zircons from prearc and postarc sequences: implications for the age of magmatism and inheritance in the Talkeetna arc. *Geol. Soc. Am. Spec. Pap.* 431:253–71
- Anderson AT. 1976. Magma mixing: petrological processes and volcanological tool. *J. Volcanol. Geotherm. Res.* 1:3–33
- Arculus RJ. 2003. Use and abuse of the terms calc-alkaline and calcalkalic. *J. Petrol.* 44:929–35
- Arculus RJ, Wills KJA. 1980. The petrology of plutonic blocks and inclusions from the Lesser Antilles island arc. *J. Petrol.* 21:743–99
- Arndt NT, Goldstein SL. 1989. An open boundary between lower continental crust and mantle: its role in crust formation and crustal recycling. *Tectonophysics* 161:201–12
- Bard JP. 1983. Metamorphism of an obducted island arc: example of the Kohistan Sequence (Pakistan) in the Himalayan collided range. *Earth Planet. Sci. Lett.* 65:133–44
- Barker F, Aleinikoff JN, Box SE, Evans BW, Gehrels GE, et al. 1994. Some accreted volcanic rocks of Alaska and their elemental abundances. In *The Geology of North America*, Vol. G-1: *The Geology of Alaska*, ed. G Plafker, HC Berg, pp. 555–87. Washington, DC: Geol. Soc. Am.
- Bassett D, Sutherland R, Henrys S, Stern T, Scherwath M, et al. 2010. Three-dimensional velocity structure of the northern Hikurangi margin, Raukumara, New Zealand: implications for the growth of continental crust by subduction erosion and tectonic underplating. *Geochim. Geophys. Geosyst.* 11:Q10013
- Bédard JH. 2006. A catalytic delamination-driven model for coupled genesis of Archean crust and sub-continental lithospheric mantle. *Geochim. Cosmochim. Acta* 70:1188–214
- Behn MD, Kelemen PB. 2006. Stability of arc lower crust: insights from the Talkeetna arc section, south central Alaska, and the seismic structure of modern arcs. *J. Geophys. Res.* 111:B11207
- Behn MD, Kelemen PB, Hirth G, Hacker BR, Massonne HJ. 2011. Diapirs as the source of the sediment signature in arc lavas. *Nat. Geosci.* 4:641–46
- Bernstein S, Kelemen PB, Hanghøj K. 2007. Consistent olivine Mg# in cratonic mantle reflects Archean mantle melting to the exhaustion of orthopyroxene. *Geology* 35:459–62
- Bignold SM, Treloar PJ, Petford N. 2006. Changing sources of magma generation beneath intra-oceanic island arcs: an insight from the juvenile Kohistan island arc, Pakistan Himalaya. *Chem. Geol.* 233:46–74
- Blatter DL, Sisson TW, Hankins WB. 2013. Crystallization of oxidized, moderately hydrous arc basalt at mid- to lower-crustal pressures: implications for andesite genesis. *Contrib. Mineral. Petrol.* 166:861–86
- Bouilhol P, Jagoutz O, Hanchar J, Dudas F. 2013. Dating the India-Eurasia collision through arc magmatic records. *Earth Planet. Sci. Lett.* 366:163–75
- Bucholz CE, Jagoutz O, Schmidt MW, Sambuu O. 2014. Phlogopite- and clinopyroxene-dominated fractional crystallization of an alkaline primitive melt: petrology and mineral chemistry of the Dariv Igneous Complex, Western Mongolia. *Contrib. Mineral. Petrol.* 167:1–28
- Burg JP. 2011. The Asia-Kohistan-India collision: review and discussion. *Front. Earth Sci.* 2011:279–309
- Burg JP, Arbaret L, Chaudhry NM, Dawood H, Hussain S, Zeilinger G. 2005. Shear strain localization from the upper mantle to the middle crust of the Kohistan Arc (Pakistan). *Geol. Soc. Lond. Spec. Publ.* 245:25–38
- Burg JP, Jagoutz O, Dawood H, Hussain SS. 2006. Precollision tilt of crustal blocks in rifted island arcs: structural evidence from the Kohistan Arc. *Tectonics* 25:TC5005
- Burns LE. 1983. *The Border Ranges ultramafic and mafic complex: plutonic core of an intraoceanic island arc*. PhD Thesis, Stanford Univ., Palo Alto, CA
- Burns LE. 1985. The Border Ranges ultramafic and mafic complex, south-central Alaska: cumulate fractionates of island-arc volcanics. *Can. J. Earth Sci.* 22:1020–38
- Burns LE, Pessel GH, Little TA, Pavlis TL, Newberry RJ, et al. 1991. *Geology of the northern Chugach Mountains, southcentral Alaska*. Prof. Rep. 94, Div. Geol. Geophys. Surv., Dep. Nat. Resour., Fairbanks, AK
- Cai Y, Rioux ME, Kelemen PB, Goldstein SL, Bolge L. 2015. Distinctly different parental magmas for calc-alkaline plutons and tholeiitic lavas in the central and eastern Aleutian arc. *Earth Planet. Sci. Lett.* Submitted

- Calvert AJ. 2011. The seismic structure of island arc crust. *Front. Earth Sci.* 2011:87–119
- Calvert AJ, Klemperer SL, Takahashi N, Kerr BC. 2008. Three-dimensional crustal structure of the Mariana island arc from seismic tomography. *J. Geophys. Res.* 113:B01406
- Chatterjee N, Jagoutz O. 2015. Exhumation of the UHP Tso Moriri eclogite as a diapir rising through the mantle wedge. *Contrib. Mineral. Petrol.* 169:3
- Christensen NI, Mooney WD. 1995. Seismic velocity structure and composition of the continental crust: a global view. *J. Geophys. Res.* 100(B6):9761–88
- Clift PD, Draut AE, Kelemen PB, Blusztajn J, Greene A, Trop J. 2005a. Stratigraphic and geochemical evolution of the Jurassic Talkeetna Volcanic Formation, south central Alaska. *Geol. Soc. Am. Bull.* 117:902–25
- Clift PD, Hannigan R, Blusztajn J, Draut AE. 2002. Geochemical evolution of the Dras-Kohistan Arc during collision with Eurasia: evidence from the Ladakh Himalaya, India. *Island Arc* 11:255–73
- Clift PD, Pavlis T, DeBari SM, Draut AE, Rioux M, Kelemen PB. 2005b. Subduction erosion of the Jurassic Talkeetna-Bonanza arc and the Mesozoic accretionary tectonics of western North America. *Geology* 33:881–84
- Clift PD, Vannucchi P. 2004. Controls on tectonic accretion versus erosion in subduction zones: implications for the origin and recycling of the continental crust. *Rev. Geophys.* 42:RG000127
- Clift PD, Vannucchi P, Morgan JP. 2009. Crustal redistribution, crust–mantle recycling and Phanerozoic evolution of the continental crust. *Earth Sci. Rev.* 97:80–104
- Cloos M, Shreve RL. 1988. Subduction-channel model of prism accretion, melange formation, sediment subduction, and subduction erosion at convergent plate margins. 1. Background and description. *Pure Appl. Geophys.* 128:455–500
- Compagnoni R, Maffeo B. 1973. Jadeite-bearing metagranites l.s. and related rocks in the Mount Mucrone area (Sesia-Lanzo Zone, western Italian Alps). *Schweiz. Mineral. Petrol. Mitt.* 53:355–77
- Connolly JAD. 1990. Multivariable phase diagrams: an algorithm based on generalized thermodynamics. *Am. J. Sci.* 290:666–718
- Connolly JAD. 2005. Computation of phase equilibria by linear programming: a tool for geodynamic modeling and its application to subduction zone decarbonation. *Earth Planet. Sci. Lett.* 236:524–41
- Conrad WK, Kay RW. 1984. Ultramafic and mafic inclusions from Adak Island: crystallization history, and implications for the nature of primary magmas and crustal evolution in the Aleutian Arc. *J. Petrol.* 25:88–125
- Conrad WK, Kay SM, Kay RW. 1983. Magma mixing in the Aleutian arc: evidence from cognate inclusions and composite xenoliths. *J. Volcanol. Geotherm. Res.* 18:279–95
- Coward MP, Jan MQ, Rex D, Tarney J, Thirlwall MF, Windley BF. 1982. Structural evolution of a crustal section in the western Himalaya. *Nature* 295:22–24
- Coward MP, Windley BF, Broughton RD, Luff IW, Petterson MG, et al. 1986. Collision tectonics in the NW Himalayas. *Geol. Soc. Lond. Spec. Publ.* 19:203–19
- Crisp JA. 1984. Rates of magma emplacement and volcanic output. *J. Volcanol. Geotherm. Res.* 20:177–211
- Chroston PN, Simmons G. 1989. Seismic velocities from the Kohistan volcanic arc, northern Pakistan. *J. Geol. Soc. Lond.* 146:971–79
- DeBari SM. 1994. Petrogenesis of the Fiambala gabbroic intrusion, northwestern Argentina, a deep crustal syntectonic pluton in a continental magmatic arc. *J. Petrol.* 35:679–713
- DeBari SM, Coleman RG. 1989. Examination of the deep levels of an island arc: evidence from the Tonsina ultramafic-mafic assemblage, Tonsina, Alaska. *J. Geophys. Res.* 94(B4):4373–91
- DeBari SM, Greene A. 2011. Vertical stratification of composition, density, and inferred magmatic processes in exposed arc crustal sections. *Front. Earth Sci.* 2011:121–44
- DeBari SM, Kay SM, Kay RW. 1987. Ultramafic xenoliths from Adagdak volcano, Adak, Aleutian islands, Alaska: deformed igneous cumulates from the Moho of an island arc. *J. Geol.* 95:329–41
- DeBari SM, Sleep NH. 1991. High-Mg, low-Al bulk composition of the Talkeetna island arc, Alaska: implications for primary magmas and the nature of arc crust. *Geol. Soc. Am. Bull.* 103:37–47
- Dhuime B, Bosch D, Bodinier JL, Garrido CJ, Bruguier O, et al. 2007. Multistage evolution of the Jijal ultramafic-mafic complex (Kohistan, N Pakistan): implications for building the roots of island arcs. *Earth Planet. Sci. Lett.* 261:179–200

- Dhuime B, Bosch D, Garrido CJ, Bodinier JL, Bruguier O, et al. 2009. Geochemical architecture of the lower-to middle-crustal section of a paleo-island arc (Kohistan complex, Jijal-Kamila area, northern Pakistan): implications for the evolution of an oceanic subduction zone. *J. Petrol.* 50:531–69
- Dick HJ, Ozawa K, Meyer PS, Niu Y, Robinson PT, et al. 2002. Primary silicate mineral chemistry of a 1.5-km section of very slow spreading lower ocean crust: ODP hole 735B, Southwest Indian Ridge. *Proc. Ocean Drill. Program Sci. Results* 176:1–61. http://www-odp.tamu.edu/publications/176_SR/chap_10/chap_10.htm
- Dimalanta C, Taira A, Yumul GP Jr, Tokuyama H, Mochizuki K. 2002. New rates of western Pacific island arc magmatism from seismic and gravity data. *Earth Planet. Sci. Lett.* 202:105–15
- Dodge FCW, Lockwood JP, Calk LC. 1988. Fragments of the mantle and crust beneath the Sierra Nevada batholith: xenoliths in a volcanic pipe near Big Creek, California. *Geol. Soc. Am. Bull.* 100:938–47
- Domenick MA, Kistler RW, Dodge FCW, Tatsumoto M. 1983. Nd and Sr isotopic study of crustal and mantle inclusions from beneath the Sierra Nevada and implications for batholith petrogenesis. *Geol. Soc. Am. Bull.* 94:713–19
- Draut AE, Clift PD. 2013. Differential preservation in the geologic record of intraoceanic arc sedimentary and tectonic processes. *Earth Sci. Rev.* 116:57–84
- Drummond MS, Defant MJ. 1990. A model for trondhjemite-tonalite-dacite genesis and crustal growth via slab melting: Archean to modern comparisons. *J. Geophys. Res.* 95(B13):21503–21
- Ducea MN, Kidder S, Chesley JT, Saleeby JB. 2009. Tectonic underplating of trench sediments beneath magmatic arcs: the central California example. *Int. Geol. Rev.* 51:1–26
- Ducea MN, Otamendi JE, Bergantz G, Stair KM, Valencia VA, Gehrels GE. 2010. Timing constraints on building an intermediate plutonic arc crustal section: U-Pb zircon geochronology of the Sierra Valle Fértil-La Huerta, Famatinian arc, Argentina. *Tectonics* 29:TC4002
- Ducea MN, Saleeby JB. 1996. Buoyancy sources for a large, unrooted mountain range, the Sierra Nevada, California: evidence from xenolith thermobarometry. *J. Geophys. Res.* 101(B4):8229–44
- Eakins BW, Sharman GF. 2012. *Hypsographic Curve of the Earth's Surface from ETOPO1*. Boulder, CO: NOAA Nat. Geophys. Data Cent.
- Fliedner MM, Klemperer SL. 1999. Structure of an island arc: wide-angle seismic studies in the eastern Aleutian Islands, Alaska. *J. Geophys. Res.* 104(B5):10667–94
- Fliedner MM, Klemperer SL, Christensen NI. 2000. Three-dimensional seismic model of the Sierra Nevada arc, California, and its implications for crustal and upper mantle composition. *J. Geophys. Res.* 105(B5):10899–921
- Frost BR, Lindsley DH. 1992. Equilibria among Fe-Ti oxides, pyroxenes, olivine, and quartz. Part II: Application. *Am. Mineral.* 77:1004–20
- Gale A, Dalton CA, Langmuir CH, Su Y, Schilling JG. 2013. The mean composition of ocean ridge basalts. *Geochem. Geophys. Geosyst.* 14:489–518
- Garrido CJ, Bodinier JL, Burg JP, Zeilinger G, Hussain SS, et al. 2006. Petrogenesis of mafic garnet granulite in the lower crust of the Kohistan paleo-arc complex (northern Pakistan): implications for intra-crustal differentiation of island arcs and generation of continental crust. *J. Petrol.* 47:1873–914
- Garrido CJ, Bodinier JL, Dhuime B, Bosch D, Chanefo I, et al. 2007. Origin of the island arc Moho transition zone via melt-rock reaction and its implications for intracrustal differentiation of island arcs: evidence from the Jijal complex (Kohistan complex, northern Pakistan). *Geology* 35:683–86
- Garrido CJ, Kelemen PB, Hirth G. 2001. Variation of cooling rate with depth in lower crust formed at an oceanic spreading ridge: plagioclase crystal size distributions in gabbros from the Oman ophiolite. *Geochem. Geophys. Geosyst.* 2:1041
- Gastil RG. 1975. Plutonic zones of the Peninsular Ranges of southern California and northern Baja California. *Geology* 3:361–63
- Gazel E, Hayes J, Hoernle K, Everson E, Holbrooke WS, et al. 2015. Continental crust generated in oceanic arcs. *Nat. Geosci.* 8:321–27
- Gerya TV, Stöckert B, Perchuk AL. 2002. Exhumation of high-pressure metamorphic rocks in a subduction channel: a numerical simulation. *Tectonics* 21:1056
- Gerya TV, Yuen DA. 2003. Rayleigh-Taylor instabilities from hydration and melting propel ‘cold plumes’ at subduction zones. *Earth Planet. Sci. Lett.* 212:47–62

- Gill JB. 1981. *Orogenic Andesites and Plate Tectonics*. Berlin: Springer-Verlag
- Godard M, Awaji S, Hansen H, Hellebrand E, Brunelli D, et al. 2009. Geochemistry of a long in-situ section of intrusive slow-spread oceanic lithosphere: results from IODP Site U1309 (Atlantis Massif, 30°N Mid-Atlantic-Ridge). *Earth Planet. Sci. Lett.* 279:110–22
- Greene A, DeBari SM, Kelemen PB, Blusztajn J, Clift PD. 2006. A detailed geochemical study of island arc crust: the Talkeetna arc section, south-central Alaska. *J. Petrol.* 47:1051–93
- Grimes CB, John BE, Kelemen PB, Mazdab FK, Wooden JL, et al. 2007. Trace element chemistry of zircons from oceanic crust: a method for distinguishing detrital zircon provenance. *Geology* 35:643–46
- Gromet LP, Silver LT. 1987. REE variations across the Peninsular Ranges batholith: implications for batholithic petrogenesis and crustal growth in magmatic arcs. *J. Petrol.* 28:75–125
- Grove M, Jacobson CE, Barth AP, Vucic A. 2003a. Temporal and spatial trends of Late Cretaceous–early Tertiary underplating of Pelona and related schist beneath southern California and southwestern Arizona. *Geol. Soc. Am. Spec. Pap.* 374:381–406
- Grove TL, Baker MB. 1984. Phase equilibrium controls on the tholeiitic versus calc-alkaline differentiation trends. *J. Geophys. Res.* 89(B5):3253–74
- Grove TL, Elkins-Tanton LT, Parman SW, Chatterjee N, Müntener O, Gaetani GA. 2003b. Fractional crystallization and mantle-melting controls on calc-alkaline differentiation trends. *Contrib. Mineral. Petrol.* 145:515–33
- Hacker BR, Kelemen PB, Behn MD. 2011. Differentiation of the continental crust by relamination. *Earth Planet. Sci. Lett.* 307:501–16
- Hacker BR, Kelemen PB, Behn MD. 2015. Continental lower crust. *Annu. Rev. Earth Planet. Sci.* 43:167–205
- Hacker BR, Mehl L, Kelemen PB, Rioux M, Behn MD, Luffi P. 2008. Reconstruction of the Talkeetna intraoceanic arc of Alaska through thermobarometry. *J. Geophys. Res.* 113:B03204
- Haraguchi S, Ishii T, Kimura JI, Ohara Y. 2003. Formation of tonalite from basaltic magma at the Komahashi-Daini Seamount, northern Kyushu-Palau Ridge in the Philippine Sea, and growth of Izu-Ogasawara (Bonin)-Mariana crust. *Contrib. Mineral. Petrol.* 145:151–68
- Hart SR, Blusztajn J, Dick HJB, Meyer PS, Muehlenbachs K. 1999. The fingerprint of seawater circulation in a 500-meter section of ocean crust gabbros. *Geochim. Cosmochim. Acta* 63:4059–80
- Hayes JL, Holbrook WS, Lizarralde D, Avendonk HJA, Bullock AD, et al. 2013. Crustal structure across the Costa Rican volcanic arc. *Geochem. Geophys. Geosyst.* 14:1087–103
- Herzberg CT, Fyfe WS, Carr MJ. 1983. Density constraints on the formation of the continental Moho and crust. *Contrib. Mineral. Petrol.* 84:1–5
- Holbrook SW, Lizarralde D, McGeary S, Bangs N, Diebold J. 1999. Structure and composition of the Aleutian island arc and implications for continental crustal growth. *Geology* 27:31–34
- Hopkins MD, Harrison TM, Manning CE. 2008. Low heat flow inferred from >4 Gyr zircons suggests Hadean plate boundary interaction. *Nature* 456:493–96
- Hopkins MD, Harrison TM, Manning CE. 2010. Constraints on Hadean geodynamics from mineral inclusions in >4 Ga zircons. *Earth Planet. Sci. Lett.* 298:367–76
- Huang Y, Chumakov V, Mantovani F, Rudnick RL, McDonough WF. 2013. A reference Earth model for the heat-producing elements and associated geoneutrino flux. *Geochem. Geophys. Geosyst.* 14:2003–29
- Ingebritsen SE, Sherrod DR, Mariner RH. 1989. Heat-flow and hydrothermal circulation in the Cascade Range, north-central Oregon. *Science* 243:1458–62
- Irvine TN, Baragar WR. 1971. A guide to the chemical classification of the common volcanic rocks. *Can. J. Earth Sci.* 8:523–48
- Iwasaki T, Hirata N, Kanazawa T, Melles J, Suyehiro K, et al. 1990. Crustal and upper mantle structure in the Ryukyu Island Arc deduced from deep seismic sounding. *Geophys. J. Int.* 102:631–51
- Iwasaki T, Yoshii T, Moriya T, Kobayashi A, Nishiwaki M, et al. 1994. Precise P and S wave velocity structures in the Kitakami massif, Northern Honshu, Japan, from a seismic refraction experiment. *J. Geophys. Res.* 99(B11):22187–204
- Jagoutz O. 2013. Were ancient granitoid compositions influenced by contemporaneous atmospheric and hydrosphere oxidation states? *Terra Nova* 25:95–101
- Jagoutz O. 2014. Arc crustal differentiation mechanisms. *Earth Planet. Sci. Lett.* 396:267–77

- Jagoutz O, Behn MD. 2013. Foundering of lower arc crust as an explanation for the origin of the continental Moho. *Nature* 504:131–34
- Jagoutz O, Müntener O, Burg JP, Ulmer P, Jagoutz E. 2006. Lower continental crust formation through focused flow in km-scale melt conduits: the zoned ultramafic bodies of the Chilas Complex in the Kohistan island arc (NW Pakistan). *Earth Planet. Sci. Lett.* 242:320–42
- Jagoutz O, Müntener O, Schmidt MW, Burg JP. 2011. The respective roles of flux and decompression melting and their relevant liquid lines of descent for continental crust formation: evidence from the Kohistan arc. *Earth Planet. Sci. Lett.* 303:25–36
- Jagoutz O, Müntener O, Ulmer P, Pettke T, Burg JP, et al. 2007. Petrology and mineral chemistry of lower crustal intrusions: the Chilas Complex, Kohistan (NW Pakistan). *J. Petrol.* 48:1895–953
- Jagoutz O, Schmidt MW. 2012. The formation and bulk composition of modern juvenile continental crust: the Kohistan arc. *Chem. Geol.* 298–99:79–96
- Jagoutz O, Schmidt MW. 2013. The composition of the foundered complement to the continental crust and a re-evaluation of fluxes in arcs. *Earth Planet. Sci. Lett.* 371–72:177–90
- Jagoutz O, Schmidt MW, Enggist A, Burg JP, Hamid D, Hussain S. 2013. TTG-type plutonic rocks formed in a modern arc batholith by hydrous fractionation in the lower arc crust. *Contrib. Mineral. Petrol.* 166:1099–118
- Jan MQ, Khan MA, Windley BF. 1989. Mineral chemistry of the Chilas mafic-ultramafic complex, Kohistan island arc, N. Pakistan: oxide phases. In *Tectonic Evolution of Collision Zones Between Gondwanic and Eurasian Blocks*, ed. MQ Jan, MJ Khan, S Hamidullah, pp. 217–39. Peshawar, Pak.: Dep. Geol., Univ. Peshawar
- Jan MQ, Khan MA, Windley BF. 1992. Exsolution in Al-Cr-Fe³⁺-rich spinels from the Chilas mafic-ultramafic complex, Pakistan. *Am. Mineral.* 77:1074–79
- Janiszewski HA, Abers GA, Shillington DJ, Calkins JA. 2013. Crustal structure along the Aleutian island arc: new insights from receiver functions constrained by active-source data. *Geochem. Geophys. Geosyst.* 14:2977–92
- Jicha BR, Jagoutz O. 2015. Magma production rates for intraoceanic arcs. *Elements* 11:105–11
- Jicha BR, Scholl DW, Singer BS, Yogodzinski GM, Kay SM. 2006. Revised age of Aleutian Island Arc formation implies high rate of magma production. *Geology* 34:661–64
- Johnsen M. 2007. *Geochemical composition of the western Talkeetna island arc crustal section, lower Cook Inlet region, Alaska: implications for crustal growth along continental margins*. MS Thesis, Western Wash. Univ., Bellingham
- Jull M, Kelemen PB. 2001. On the conditions for lower crustal convective instability. *J. Geophys. Res.* 106(B4):6423–46
- Karig DE. 1971. Structural history of the Mariana island arc system. *Geol. Soc. Am. Bull.* 82:323–44
- Kawate S. 1996. *Geochemical models of the oceanic island arc system: an example of the Tanzawa Mountainland, central Japan*. PhD Thesis, Tohoku Univ., Tohoku, Jpn.
- Kawate S, Arima M. 1998. Petrogenesis of the Tanzawa plutonic complex, central Japan: exposed felsic middle crust of the Izu-Bonin-Mariana arc. *Island Arc* 7:342–58
- Kay RW. 1978. Aleutian magnesian andesites: melts from subducted Pacific Ocean crust. *J. Volcanol. Geotherm. Res.* 4:117–32
- Kay RW, Kay SM. 1991. Creation and destruction of lower continental crust. *Geol. Rundsch.* 80:259–78
- Kay SM, Kay RW, Perfit MR. 1990. Calc-alkaline plutonism in the intra-oceanic Aleutian arc, Alaska. *Geol. Soc. Am. Spec. Pap.* 241:233–55
- Kelemen PB. 1995. Genesis of high Mg# andesites and the continental crust. *Contrib. Mineral. Petrol.* 120:1–19
- Kelemen PB, Behn MD. 2015. Genesis of continental crust via density sorting in subducted arcs. *Nat. Geosci.* In revision
- Kelemen PB, Ghiorso MS. 1986. Assimilation of peridotite in zoned calc-alkaline plutonic complexes: evidence from the Big Jim complex, Washington Cascades. *Contrib. Mineral. Petrol.* 94:12–28
- Kelemen PB, Hacker BR, Behn MD, Greene A, Rioux M, et al. 2015. Possible bulk compositions for the Talkeetna arc: 50 to 62 wt% SiO₂. *Geology*. In preparation
- Kelemen PB, Hanghøj K, Greene A. 2004. One view of the geochemistry of subduction-related magmatic arcs, with an emphasis on primitive andesite and lower crust. In *Treatise on Geochemistry*, Vol. 3: *The Crust*, ed. RL Rudnick, pp. 593–659. Oxford, UK: Pergamon. 1st ed.

- Kelemen PB, Hanghøj K, Greene A. 2014. One view of the geochemistry of subduction-related magmatic arcs, with an emphasis on primitive andesite and lower crust. In *Treatise on Geochemistry*, Vol. 4: *The Crust*, ed. RL Rudnick, pp. 746–805. Oxford, UK: Pergamon. 2nd ed.
- Kelemen PB, Hart SR, Bernstein S. 1998. Silica enrichment in the continental upper mantle lithosphere via melt/rock reaction. *Earth Planet. Sci. Lett.* 164:387–406
- Kelemen PB, Kikawa E, Miller DJ, Shipboard Sci. Party. 2007. Leg 209 summary: processes in a 20-km-thick conductive boundary layer beneath the Mid-Atlantic Ridge, 14°–16°N. *Proc. Ocean Drill. Program Sci. Results* 209:1–33. http://www-odp.tamu.edu/publications/209_SR/summary/summary.htm
- Kelemen PB, Rilling JL, Parmentier EM, Mehl L, Hacker BR. 2003a. Thermal structure due to solid-state flow in the mantle wedge beneath arcs. *AGU Monogr.* 138:293–311
- Kelemen PB, Yogodzinski GM, Scholl DW. 2003b. Along-strike variation in lavas of the Aleutian island arc: implications for the genesis of high Mg# andesite and the continental crust. *AGU Monogr.* 138:223–76
- Khan MA, Jan MQ, Weaver BL. 1993. Evolution of the lower arc crust in Kohistan, N. Pakistan: temporal arc magmatism through early, mature and intra-arc rift stages. *Geol. Soc. Lond. Spec. Publ.* 74:123–38
- Khan MA, Jan MQ, Windley BF, Tarney J, Thirlwall MF. 1989. The Chilas mafic-ultramafic igneous complex: the root of the Kohistan island arc in the Himalaya of northern Pakistan. *Geol. Soc. Am. Spec. Pap.* 232:75–94
- Khan SD, Walker DJ, Hall SA, Burke KC, Shah MT, Stockli L. 2009. Did the Kohistan-Ladakh island arc collide first with India? *Geol. Soc. Am. Bull.* 121:366–84
- Kiddle EJ, Edwards BR, Loughlin SC, Petterson M, Sparks RSJ, Voight B. 2010. Crustal structure beneath Montserrat, Lesser Antilles, constrained by xenoliths, seismic velocity structure and petrology. *Geophys. Res. Lett.* 37:L00E11
- Kodaira S, Sato T, Takahashi N, Ito A, Tamura Y, et al. 2007a. Seismological evidence for variable growth of crust along the Izu intraoceanic arc. *J. Geophys. Res.* 112:B05104
- Kodaira S, Sato T, Takahashi N, Miura S, Tamura Y, et al. 2007b. New seismological constraints on growth of continental crust in the Izu-Bonin intra-oceanic arc. *Geology* 35:1031–34
- Kopp H, Weinzierl W, Becel A, Charvis P, Evain M, et al. 2011. Deep structure of the central Lesser Antilles Island Arc: relevance for the formation of continental crust. *Earth Planet. Sci. Lett.* 304:121–34
- Lee CT, Cheng X, Horodyskyj U. 2006. The development and refinement of continental arcs by primary basaltic magmatism, garnet pyroxenite accumulation, basaltic recharge and delamination: insights from the Sierra Nevada, California. *Contrib. Mineral. Petrol.* 151:222–42
- Lee CT, Morton DM, Kistler RW, Baird AK. 2007. Petrology and tectonics of Phanerozoic continent formation: from island arcs to accretion and continental arc magmatism. *Earth Planet. Sci. Lett.* 263:370–87
- Lee CT, Morton DM, Little MG, Kistler R, Horodyskyj UN, et al. 2008. Regulating continent growth and composition by chemical weathering. *PNAS* 105:4981–86
- Little T, Hacker B, Gordon S, Baldwin S, Fitzgerald P, et al. 2011. Diapiric exhumation of Earth's youngest (UHP) eclogites in the gneiss domes of the D'Entrecasteaux Islands, Papua New Guinea. *Tectonophysics* 510:39–68
- MacLeod CJ, Lissenberg CJ, Bibby LE. 2013. 'Moist MORB' axial magmatism in the Oman ophiolite: the evidence against a mid-ocean ridge origin. *Geology* 41:459–62
- MacLeod CJ, Yaouancq G. 2000. A fossil melt lens in the Oman ophiolite: implications for magma chamber processes at fast spreading ridges. *Earth Planet. Sci. Lett.* 176:357–73
- Malaviarachchi SPK, Makishima A, Tanimoto M, Kuritani T, Nakamura E. 2008. Highly unradiogenic lead isotope ratios from the Horoman peridotite in Japan. *Nat. Geosci.* 1:859–63
- Martin H. 1986. Effect of steeper Archean geothermal gradient on geochemistry of subduction-zone magmas. *Geology* 14:753–56
- McDonough WF, Sun SS. 1995. The composition of the Earth. *Chem. Geol.* 120:223–53
- McLennan SM, Taylor SR, McCullough MT, Maynard JB. 1990. Geochemical and Nd-Sr isotopic composition of deep sea turbidites: crustal evolution and plate tectonic associations. *Geochim. Cosmochim. Acta* 54:2015–50
- Mehl L, Hacker BR, Hirth G, Kelemen PB. 2003. Arc-parallel flow within the mantle wedge: evidence from the accreted Talkeetna arc, south central Alaska. *J. Geophys. Res.* 108(B8):2375

- Miller DJ, Christensen NI. 1994. Seismic signature and geochemistry of an island arc: a multidisciplinary study of the Kohistan accreted terrane, northern Pakistan. *J. Geophys. Res.* 99(B6):11623–42
- Miller DJ, Loucks RR, Ashraf M. 1991. Platinum-group element mineralization in the Jijal layered ultramafic-mafic complex, Pakistani Himalayas. *Econ. Geol.* 86:1093–102
- Miller NC, Behn MD. 2012. Timescales for the growth of sediment diapirs in subduction zones. *Geophys. J. Int.* 190:1361–77
- Miyashiro A. 1974. Volcanic rock series in island arcs and active continental margins. *Am. J. Sci.* 274:321–55
- Müntener O, Kelemen PB, Grove TL. 2001. The role of H₂O during crystallization of primitive arc magmas under uppermost mantle conditions and genesis of igneous pyroxenites: an experimental study. *Contrib. Mineral. Petrol.* 141:643–58
- Nakanishi A, Kurashimo E, Tatsumi Y, Yamaguchi H, Miura S, et al. 2009. Crustal evolution of the southwestern Kuril Arc, Hokkaido Japan, deduced from seismic velocity and geochemical structure. *Tectonophysics* 472:105–23
- Newberry R, Burns L, Pessel P. 1986. Volcanogenic massive sulfide deposits and the missing complement to the calc-alkaline trend: evidence from the Jurassic Talkeetna island arc of southern Alaska. *Econ. Geol.* 81:951–60
- Otamendi JE, Ducea MN, Bergantz GW. 2012. Geological, petrological and geochemical evidence for progressive construction of an arc crustal section, Sierra de Valle Fértil, Famatinian Arc, Argentina. *J. Petrol.* 52:761–800
- Otamendi JE, Ducea MN, Tibaldi AM, Bergantz GW, de la Rosa J, Vujovich GI. 2009. Generation of tonalitic and dioritic magmas by coupled partial melting of gabbroic and metasedimentary rocks within the deep crust of the Famatinian magmatic arc, Argentina. *J. Petrol.* 50:841–73
- Parkinson IJ, Arculus RJ, Eggins SM. 2003. Peridotite xenoliths from Grenada, Lesser Antilles island arc. *Contrib. Mineral. Petrol.* 146:241–62
- Pearce JA, Alabaster T, Shelton AW, Searle MP. 1981. The Oman ophiolite as a Cretaceous arc-basin complex: evidence and implications. *Philos. Trans. R. Soc. A* 300:299–317
- Petterson MG, Treloar PJ. 2004. Volcanostratigraphy of arc volcanic sequences in the Kohistan arc, North Pakistan: volcanism within island arc, back-arc-basin, and intra-continental tectonic settings. *J. Volcanol. Geotherm. Res.* 130:147–78
- Petterson MG, Windley BF. 1985. Rb-Sr dating of the Kohistan arc-batholith in the Trans-Himalaya of North Pakistan, and tectonic implications. *Earth Planet. Sci. Lett.* 74:45–57
- Petterson MG, Windley BF. 1991. Changing source regions of magmas and crustal growth in the Trans-Himalayas: evidence from the Chalt Volcanics and Kohistan Batholith, Kohistan, northern Pakistan. *Earth Planet. Sci. Lett.* 102:326–41
- Petterson MG, Windley BF, Luff IW. 1991. The Chalt Volcanics, Kohistan, N Pakistan; high-Mg tholeiitic and low-Mg calc-alkaline volcanism in a Cretaceous island arc. *Phys. Chem. Earth* 17:19–30
- Peucker-Ehrenbrink B, Hanghøj K, Atwood T, Kelemen PB. 2012. Rhenium-osmium isotope systematics and platinum group element concentrations in oceanic crust. *Geology* 40:199–202
- Plafker G, Nokleberg WJ, Lull JS. 1989. Bedrock geology and tectonic evolution of the Wrangellia, Peninsular, and Chugach terranes along the trans-Alaska crustal transect in the Chugach Mountains and Southern Copper River Basin, Alaska. *J. Geophys. Res.* 94(B4):4255–95
- Plank T. 2005. Constraints from thorium/lanthanum on sediment recycling at subduction zones and the evolution of the continents. *J. Petrol.* 46:921–44
- Rapp RP, Watson EB. 1995. Dehydration melting of metabasalt at 8–32 kbar: implications for continental growth and crust–mantle recycling. *J. Petrol.* 36:891–931
- Rapp RP, Watson EB, Miller CF. 1991. Partial melting of amphibolite/eclogite and the origin of Archean trondhjemites and tonalites. *Precambrian Res.* 51:1–25
- Reymer A, Schubert G. 1984. Phanerozoic addition rates to the continental crust and crustal growth. *Tectonics* 3:63–77
- Ringuette L, Martignole J, Windley BF. 1999. Magmatic crystallization, isobaric cooling, and decompression of the garnet-bearing assemblages of the Jijal Sequence (Kohistan Terrane, western Himalayas). *Geology* 27:139–42

- Ringwood AE, Green DH. 1966. An experimental investigation of the gabbro-eclogite transformation and some geophysical implications. *Tectonophysics* 3:383–427
- Rioux M. 2006. *The growth and differentiation of arc crust: temporal and geochemical evolution of the accreted Talkeetna arc, south-central Alaska*. PhD Thesis, Univ. Calif., Santa Barbara
- Rioux M, Hacker B, Mattinson J, Kelemen P, Blusztajn J, Gehrels G. 2007. Magmatic development of an intra-oceanic arc: high-precision U-Pb zircon and whole-rock isotopic analyses from the accreted Talkeetna arc, south-central Alaska. *Geol. Soc. Am. Bull.* 119:1168–84
- Rioux M, Mattinson J, Hacker B, Kelemen P, Blusztajn J, et al. 2010. Intermediate to felsic middle crust in the accreted Talkeetna arc, the Alaska Peninsula and Kodiak island, Alaska: an analogue for low-velocity middle crust in modern arcs. *Tectonics* 29:TC3001
- Rosing MT, Bird DK, Sleep NH, Glassley W, Albarede F. 2006. The rise of continents: an essay on the geologic consequences of photosynthesis. *Palaeogeogr. Palaeoclimatol. Palaeoecol.* 232:99–113
- Rudnick RL, Gao S. 2004. Composition of the continental crust. In *Treatise on Geochemistry*, Vol. 3: *The Crust*, ed. RL Rudnick, pp. 1–64. Oxford, UK: Pergamon. 1st ed.
- Rudnick RL, Gao S. 2014. Composition of the continental crust. In *Treatise on Geochemistry*, Vol. 4: *The Crust*, ed. RL Rudnick, pp. 1–51. Oxford, UK: Pergamon. 2nd ed.
- Rudnick RL, Presper T. 1990. Geochemistry of intermediate- to high-pressure granulites. *NATO Sci. Ser. C* 311:523–50
- Saito S, Arima M, Nakajima T, Misawa K, Kimura JI. 2007. Formation of distinct granitic magma batches by partial melting of hybrid lower crust in the Izu arc collision zone, Central Japan. *J. Petrol.* 48:1761–91
- Saleeby J, Ducea M, Clemens-Knott D. 2003. Production and loss of high-density batholithic root, southern Sierra Nevada, California. *Tectonics* 22:1064
- Schaltegger U, Zeilinger G, Frank M, Burg JP. 2002. Multiple mantle sources during island arc magmatism: U-Pb and Hf isotopic evidence from the Kohistan arc complex, Pakistan. *Terra Nova* 14:461–68
- Scherwath M, Kopp H, Flueh ER, Henrys SA, Sutherland R, et al. 2010. Fore-arc deformation and underplating at the northern Hikurangi margin, New Zealand. *J. Geophys. Res.* 115:B06408
- Searle MP, Khan MA, Fraser JE, Gough SJ, Qasim JM. 1999. The tectonic evolution of the Kohistan-Karakoram collision belt along the Karakoram Highway transect, North Pakistan. *Tectonics* 18:929–49
- Sharp ZD, Essene EJ, Smyth JR. 1992. Ultra-high temperatures from oxygen isotope thermometry of a coesite-sanidine grosspyrite. *Contrib. Mineral. Petrol.* 112:358–70
- Shillington DJ, Van Avendonk HJA, Behn MD, Kelemen PB, Jagoutz O. 2013. Constraints on the composition of the Aleutian arc lower crust from V_p/V_s . *Geophys. Res. Lett.* 40:2579–84
- Shillington DJ, Van Avendonk HJA, Holbrook WS, Kelemen PB, Hornbach MJ. 2004. Composition and structure of the central Aleutian island arc from arc-parallel wide-angle seismic data. *Geochem. Geophys. Geosyst.* 5:Q10006
- Shipboard Sci. Party. 2004. Leg 209 summary. *Proc. Ocean Drill. Program Initial Rep.* 209:1–139. http://www-odp.tamu.edu/publications/209_IR/chap_01/chap_01.htm
- Silver LT, Chappell BW. 1988. The Peninsular Ranges batholith: an insight into the evolution of the Cordilleran batholiths of southwestern North America. *Trans. R. Soc. Edinb. Earth Sci.* 79:105–21
- Sisson TW, Grove TL, Coleman DS. 1996. Hornblende gabbro sill complex at Onion Valley, California, and a mixing origin for the Sierra Nevada batholith. *Contrib. Mineral. Petrol.* 126:81–108
- Stern RJ. 1979. On the origin of andesite in the northern Mariana Island Arc: implications from Agrigan. *Contrib. Mineral. Petrol.* 68:207–19
- Suyehiro K, Takahashi N, Arie Y, Yokoi Y, Hino R, et al. 1996. Continental crust, crustal underplating, and low- Q upper mantle beneath an oceanic island arc. *Science* 272:390–92
- Tahirikheli RAK. 1979. Geology of Kohistan and adjoining Eurasia and Indio-Pakistan continents, Pakistan. *Geol. Bull. Univ. Peshawar* 11:1–30
- Takahashi N, Kodaira S, Klemperer S, Tatsumi Y, Kaneda Y, Suyehiro K. 2007. Crustal structure and evolution of the Mariana intra-oceanic island arc. *Geology* 35:203–6
- Takahashi N, Kodaira S, Tatsumi Y, Kaneda Y, Suyehiro K. 2008. Structure and growth of the Izu-Bonin-Mariana arc crust. 1: Seismic constraint on crust and mantle structure of the Mariana arc-back-arc system. *J. Geophys. Res.* 113:B01104

- Takahashi N, Kodaira S, Tatsumi Y, Yamashita M, Sato T, et al. 2009. Structural variations of arc crusts and rifted margins in the southern Izu-Ogasawara arc-back arc system. *Geochem. Geophys. Geosyst.* 10:Q09X08
- Tamura Y, Ishizuka O, Aoike K, Kawate S, Kawabata H, et al. 2010. Missing Oligocene crust of the Izu-Bonin arc: consumed or rejuvenated during collision? *J. Petrol.* 51:823–46
- Tani K, Fiske RS, Dunkley DJ, Ishizuka O, Oikawa T, et al. 2011. The Izu Peninsula, Japan: zircon geochronology reveals a record of intra-oceanic rear-arc magmatism in an accreted block of Izu-Bonin upper crust. *Earth Planet. Sci. Lett.* 303:225–39
- Tatsumi Y. 2000. Continental crust formation by crustal delamination in subduction zones and complementary accumulation of the enriched mantle I component in the mantle. *Geochem. Geophys. Geosyst.* 1:1053
- Tatsumi Y, Shukuno H, Tani K, Takahashi N, Kodaira S, Kogiso T. 2008. Structure and growth of the Izu-Bonin-Mariana arc crust. 2: Role of crust-mantle transformation and the transparent Moho in arc crust evolution. *J. Geophys. Res.* 113:B02203
- Taylor SR, McLennan SM. 1985. *The Continental Crust: Its Composition and Evolution*. Oxford, UK: Blackwell
- Taylor SR, McLennan SM. 1995. The geochemical evolution of the continental crust. *Rev. Geophys.* 33:241–65
- Tollan PME, Bindeman I, Blundy JD. 2012. Cumulate xenoliths from St. Vincent, Lesser Antilles Island Arc: a window into upper crustal differentiation of mantle-derived basalts. *Contrib. Mineral. Petrol.* 163:189–208
- Treloar PJ, Brodie KH, Coward MP, Jan MQ, Khan MA, et al. 1990. The evolution of the Kamila shear zone, Kohistan, Pakistan. *NATO Sci. Ser. C* 317:175–214
- Treloar PJ, Petterson MG, Jan MQ, Sullivan MA. 1996. A re-evaluation of the stratigraphy and evolution of the Kohistan Arc sequence, Pakistan Himalaya: implications for magmatic and tectonic arc-building processes. *J. Geol. Soc. Lond.* 153:681–93
- Trop JM, Szuch DA, Rioux M, Blodgett RB. 2005. Sedimentology and provenance of the Upper Jurassic Naknek Formation, Talkeetna Mountains, Alaska: bearings on the accretionary tectonic history of the Wrangellia composite terrane. *Geol. Soc. Am. Bull.* 117:570–88
- Vera E, Mutter J, Buhl P, Orcutt J, Harding A, et al. 1990. The structure of 0- to 0.2-m.y.-old oceanic crust at 9°N on the East Pacific Rise from expanded spread profiles. *J. Geophys. Res.* 95(B10):15529–56
- von Huene R, Scholl DW. 1991. Observations at convergent margins concerning sediment subduction, subduction erosion, and the growth of continental crust. *Rev. Geophys.* 29:279–316
- Walsh EO, Hacker BR. 2004. The fate of subducted continental margins: two-stage exhumation of the high-pressure to ultrahigh-pressure Western Gneiss complex, Norway. *J. Metamorph. Geol.* 22:671–89
- Warren CJ, Beaumont C, Jamieson RA. 2008. Modelling tectonic styles and ultrahigh pressure (UHP) rock exhumation during the transition from oceanic subduction to continental collision. *Earth Planet. Sci. Lett.* 267:129–45
- Warren JM, Shirey SB. 2012. Pb and Os isotopic constraints on the oceanic mantle from single abyssal peridotite sulfides. *Earth Planet. Sci. Lett.* 359–60:279–93
- Weaver BL, Tarney J. 1984. Empirical approach to estimating the composition of the continental crust. *Nature* 310:575–77
- Wedepohl KH. 1995. The composition of the continental crust. *Geochim. Cosmochim. Acta* 59:1217–32
- Wernicke B, Clayton R, Ducea M, Jones CH, Park S, et al. 1996. Origin of high mountains in the continents: the southern Sierra Nevada. *Science* 271:190–93
- Whitney DL, Teyssier C, Rey PF. 2009. The consequences of crustal melting in continental subduction. *Lithosphere* 1:323–27
- Yamamoto H, Kobayashi K, Nakamura E, Kaneko Y, Kausar AB. 2005. U-Pb zircon dating of regional deformation in the lower crust of the Kohistan arc. *Int. Geol. Rev.* 47:1035–47
- Yamamoto H, Yoshino T. 1998. Superposition of replacements in the mafic granulites of the Jijal Complex of the Kohistan Arc, northern Pakistan; dehydration and rehydration within deep arc crust. *Lithos* 43:219–34
- Yaouancq G, MacLeod CJ. 2000. Petrofabric investigation of gabbros from the Oman ophiolite: comparison between AMS and rock fabric. *Mar. Geophys. Res.* 21:289–305
- Yogodzinski GM, Kay RW, Volynets ON, Koloskov AV, Kay SM. 1995. Magnesian andesite in the western Aleutian Komandorsky region: implications for slab melting and processes in the mantle wedge. *Geol. Soc. Am. Bull.* 107:505–19

- Yogodzinski GM, Kelemen PB. 2000. Geochemical diversity in primitive Aleutian magmas: evidence from an ion probe study of clinopyroxene in mafic and ultramafic xenoliths. *Eos Trans. AGU* 81(Fall Meet. Suppl.):F1281 (Abstr.)
- Yogodzinski GM, Kelemen PB. 2007. Trace elements in clinopyroxenes from Aleutian xenoliths: implications for primitive subduction magmatism in an island arc. *Earth Planet. Sci. Lett.* 256:617–32
- Yogodzinski GM, Volynets ON, Koloskov AV, Seliverstov NI, Matvenkov VV. 1994. Magnesian andesites and the subduction component in a strongly calc-alkaline series at Piip Volcano, far Western Aleutians. *J. Petrol.* 35:163–204
- Yoshino T, Okudaira T. 2004. Crustal growth by magmatic accretion constrained by metamorphic P – T paths and thermal models of the Kohistan arc, NW Himalayas. *J. Petrol.* 45:2287–302
- Yoshino T, Yamamoto H, Okudaira T, Toriumi M. 1998. Crustal thickening of the lower crust of the Kohistan Arc (N. Pakistan) deduced from Al zoning in clinopyroxene and plagioclase. *J. Metamorph. Geol.* 16:729–48
- Zaman H, Torii M. 1999. Palaeomagnetic study of Cretaceous red beds from the eastern Hindukush ranges, northern Pakistan: palaeoreconstruction of the Kohistan–Karakoram composite unit before the India–Asia collision. *Geophys. J. Int.* 136:719–38
- Zeitler PK. 1985. Cooling history of the NW Himalaya, Pakistan. *Tectonics* 4:127–51
- Zhang SQ, Mahoney JJ, Mo XX, Ghazi AM, Milani L, et al. 2005. Evidence for a widespread Tethyan upper mantle with Indian–Ocean-type isotopic characteristics. *J. Petrol.* 46:829–58
- Zonenshain L, Kuzmin M. 1978. The Khan–Taishir ophiolitic complex of western Mongolia, its petrology, origin and comparison with other ophiolitic complexes. *Contrib. Mineral. Petrol.* 67:95–109

Contents

A Conversation with James J. Morgan <i>James J. Morgan and Dianne K. Newman</i>	1
Global Monsoon Dynamics and Climate Change <i>An Zhibeng, Wu Guoxiong, Li Jianping, Sun Youbin, Liu Yimin, Zhou Weijian, Cai Yanjun, Duan Anmin, Li Li, Mao Jiangyu, Cheng Hai, Shi Zhengguo, Tan Liangcheng, Yan Hong, Ao Hong, Chang Hong, and Feng Juan</i>	29
Conservation Paleobiology: Leveraging Knowledge of the Past to Inform Conservation and Restoration <i>Gregory P. Dietl, Susan M. Kidwell, Mark Brenner, David A. Burney, Karl W. Flessa, Stephen T. Jackson, and Paul L. Koch</i>	79
Jadeitites and Plate Tectonics <i>George E. Harlow, Tatsuki Tsujimori, and Sorena S. Sorensen</i>	105
Macroevolutionary History of the Planktic Foraminifera <i>Andrew J. Fraass, D. Clay Kelly, and Shanan E. Peters</i>	139
Continental Lower Crust <i>Bradley R. Hacker, Peter B. Kelemen, and Mark D. Behn</i>	167
Oceanic Forcing of Ice-Sheet Retreat: West Antarctica and More <i>Richard B. Alley, Sridhar Anandakrishnan, Knut Christianson, Huw J. Horgan, Atsu Muto, Byron R. Parizek, David Pollard, and Ryan T. Walker</i>	207
From Geodetic Imaging of Seismic and Aseismic Fault Slip to Dynamic Modeling of the Seismic Cycle <i>Jean-Philippe Avouac</i>	233
The Pyrogenic Carbon Cycle <i>Michael I. Bird, Jonathan G. Wynn, Gustavo Saiz, Christopher M. Wurster, and Anna McBeath</i>	273
The Architecture, Chemistry, and Evolution of Continental Magmatic Arcs <i>Mibai N. Ducea, Jason B. Saleeby, and George Bergantz</i>	299
Paleosols as Indicators of Paleoenvironment and Paleoclimate <i>Neil J. Tabor and Timothy S. Myers</i>	333

Role of Arc Processes in the Formation of Continental Crust <i>Oliver Jagoutz and Peter B. Kelemen</i>	363
Environment and Climate of Early Human Evolution <i>Naomi E. Levin</i>	405
Magma Fragmentation <i>Helge M. Gonnermann</i>	431
Atmospheric Escape from Solar System Terrestrial Planets and Exoplanets <i>Feng Tian</i>	459
A Tale of Amalgamation of Three Permo-Triassic Collage Systems in Central Asia: Oroclines, Sutures, and Terminal Accretion <i>Wenjiao Xiao, Brian F. Windley, Shu Sun, Jiliang Li, Baochun Huang, Chunming Han, Chao Yuan, Min Sun, and Hanlin Chen</i>	477
Atmospheric Dynamics of Hot Exoplanets <i>Kevin Heng and Adam P. Showman</i>	509
Transient Creep and Strain Energy Dissipation: An Experimental Perspective <i>Ulrich Faul and Ian Jackson</i>	541
Rapid Plate Motion Variations Through Geological Time: Observations Serving Geodynamic Interpretation <i>Giampiero Iaffaldano and Hans-Peter Bunge</i>	571
Rethinking the Ancient Sulfur Cycle <i>David A. Fike, Alexander S. Bradley, and Catherine V. Rose</i>	593

Indexes

Cumulative Index of Contributing Authors, Volumes 34–43	623
Cumulative Index of Article Titles, Volumes 34–43	628

Errata

An online log of corrections to *Annual Review of Earth and Planetary Sciences* articles
may be found at <http://www.annualreviews.org/errata/earth>